



THE UNIVERSITY OF
WARWICK

Department of Chemistry/ MOAC Doctoral Centre

Thesis submitted for the part of the degree of MSc in Mathematical
Biology and Biophysical Chemistry.

**Solid –state ^{13}C NMR studies of the immobilization of plant
hormones on photoreactive supports**

Prakash Patel

Supervisors: Steven Brown & Andrew Marsh

Table of Contents

Acknowledgements	ii
Summary.....	iii
Introduction	1
Basics of NMR Spectroscopy.....	5
¹³ C CP MAS Solid-State NMR Spectroscopy (¹ H decoupled)	8
The chemistry of the photoreactive tags.....	11
Materials and Methods	14
Infrared Spectroscopy.....	16
Solid-State MAS NMR spectroscopy.....	16
¹³ C NMR prediction	17
Results and Discussion	18
Sample 1 - SJD-IV-707 + glutathione + water	18
Sample 2 - SJD-IV-707 (unreacted)	18
Sample 3 – Thiourea silica azide (unreacted).....	19
Sample 4 – Thiourea silica azide + glutathione + water	20
Sample 5 – Thiourea silica azide + IAA + water	25
Sample 6 – Thiourea silica azide + IAA + DMSO.....	26
Sample 7 – Thiourea silica azide + ABA + water + 20 drops DMSO	26
Sample 8 – Peptide silica azide + glutathione	27
Sample 9 – Thiourea silica azide + water.....	29
Conclusions	31
Suggestions for further work	31
References	33
Appendix	35
Abbreviations	44

Acknowledgements

I would like to thank my supervisors Dr. Andrew Marsh and Dr. Steven Brown for their guidance and support throughout the duration of this project. Special thanks go to my regular supervisor Dr. Suzanne Dilly for her expert guidance in the laboratory, and to John Griffin in Physics, whose general guidance and helpfulness was greatly appreciated in operating one of the most expensive and difficult pieces of instrument, the solid-state NMR spectrometer.

Above all I would like to thank my family, Bugadoo, Fluffy and company for their continued guidance and support throughout my degree, and to the MOAC board and EPSRC Life Sciences Interface for giving me the opportunity to expand the scope of my work beyond my pure mathematics background.

P.P,
July 2005.

Summary

The immobilization of small molecules onto protein-resistant surfaces is important in many biological applications, from elucidating protein-substrate reactions to novel drug discovery. At Warwick, a system of photoreactive tags have been developed, which the small molecule of interest can be immobilised in solution by the exposure of light, and have been used to immobilize the small biological molecules to discover new protein interactions via phage display.

As protein interactions with small molecules are specific, it is essential to characterise the modes of attachment of these small molecules to the photoreactive tags to interpret the results of these biological analyses. In this study, silica bead-supported phenyl azide and trifluoromethyldiazirine which comprise part of the photoreactive tags used in the MagicTag™ system were reacted with glutathione, indole acetic acid (IAA) and abscisic acid (ABA), using ^{13}C solid-state nuclear magnetic spectroscopy and infrared spectroscopy.

The sample of silica bead-supported trifluoromethyldiazirine was found to be faulty, hence was not studied any further.

The silica-supported phenyl azide was found to attach to glutathione readily via an azo bond to its N-terminus amino group, and probably some C-H bond insertion to form a secondary amine, but also the primary amine group replacing the azide was also a prominent reaction, which hydrogen atoms are abstracted from the glutathione and corresponds to no insertion of glutathione in this case. Another type of silica-supported phenyl azide was found to react with glutathione similarly, with less azo bond formation and more primary amine production.

The reaction of silica-supported phenyl azide with IAA and ABA was poor (although there is some evidence of formation of an amido bond with these two compounds), and in the case of IAA was not due to the concentration of the solution used nor the absorbance of light at the azide activation frequency.

Introduction

The importance of certain small molecules in biology has long been acknowledged, but the mechanisms and ways they affect cellular metabolism is still a mystery for many of these molecules.

Small chemical molecules are efficient in selectively perturbing cellular signalling and the functions of biological targets, for example genes and proteins (Uttamchandani, Walsh et al. 2005). To find the role of small molecules in an organism it is necessary to characterise its interactions with cellular proteins. The immobilization of small molecules onto surfaces is very important for this use from its use in small molecule microarrays (SMMs) and in the construction of assay material.

SMMs are composed of many small molecules that are immobilised into separate wells (analogous to oligonucleotide microarrays which are used to characterise the mRNAs present in a cell). These can be used in the detection of binding or enzymic activity of a protein against the small molecules; the main use of this is to find novel compounds for drug development.

Small molecules attached to a surface in an assay can be used for detecting and purifying of proteins that bind to them, which combines affinity chromatography with amplification of the material. In the case of the phage display technique, the proteins are displayed on a phage vector and amplification is achieved by infecting *Escherichia coli* with the phages.

At Warwick, the MagicTag™ system has been developed (Fig. 1), in which several types of photoreactive probes immobilize the chemical in solution to a silica surface on exposure to ultraviolet or visible light, specifically for use with the phage display biopanning technique.

The aim of using many different probes is to immobilize the chemical in as many ways as possible, so that all possible binding sites are exposed, but some modes of attachment will be more favourable than others depending on the chemistry of the photoreactive tags. As the binding of the protein to the molecule is specific, there is a great need to find out which parts of the molecule are exposed because if the molecule is oriented differently this may give different conclusions about which protein receptors are most effective.

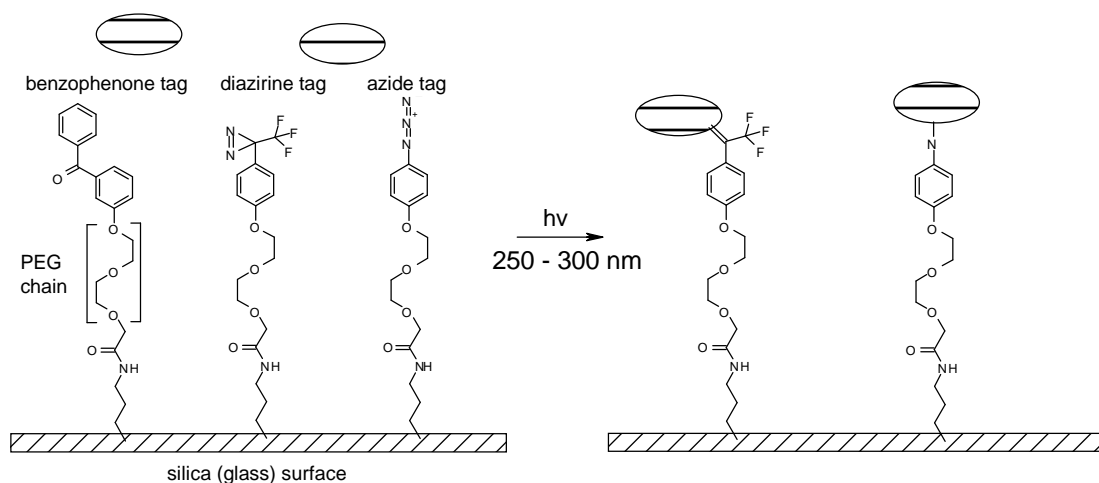


Figure 1: Some examples of MagicTag™ photoreactive tags supported on a silica surface. To immobilize small molecules (represented by ovals) in solution, the tags are activated by light and react with the small molecules (and solution). The PEG (polyethylene glycol) chain on each of the tags is electron-rich; this has a repellent effect and helps to minimize non-specific binding to the tags and silica support.

Phage display is an *in vitro* technique which allows the expression, selection and subsequent amplification of proteins on the surface of bacteriophage viral particles. Complementary DNA (cDNA) corresponding to the required proteins (either from a library of putative genes or from reverse transcribed mRNA of a cell) to display on the viral coat of the phage is inserted into the phage coat protein gene. These are then packaged into viral particles for infection into a colony of *E. coli* to produce bacteriophages which display one copy of a protein on their coat.

These phages are washed in an affinity column of immobilised small molecules such that only phages which bind specifically with the small molecules are left in the column, which are extracted and reinfected into *E. coli* to amplify them. This process is repeated a few times, which afterwards the proteins are identified by sequencing the coat protein genes of the purified viruses.

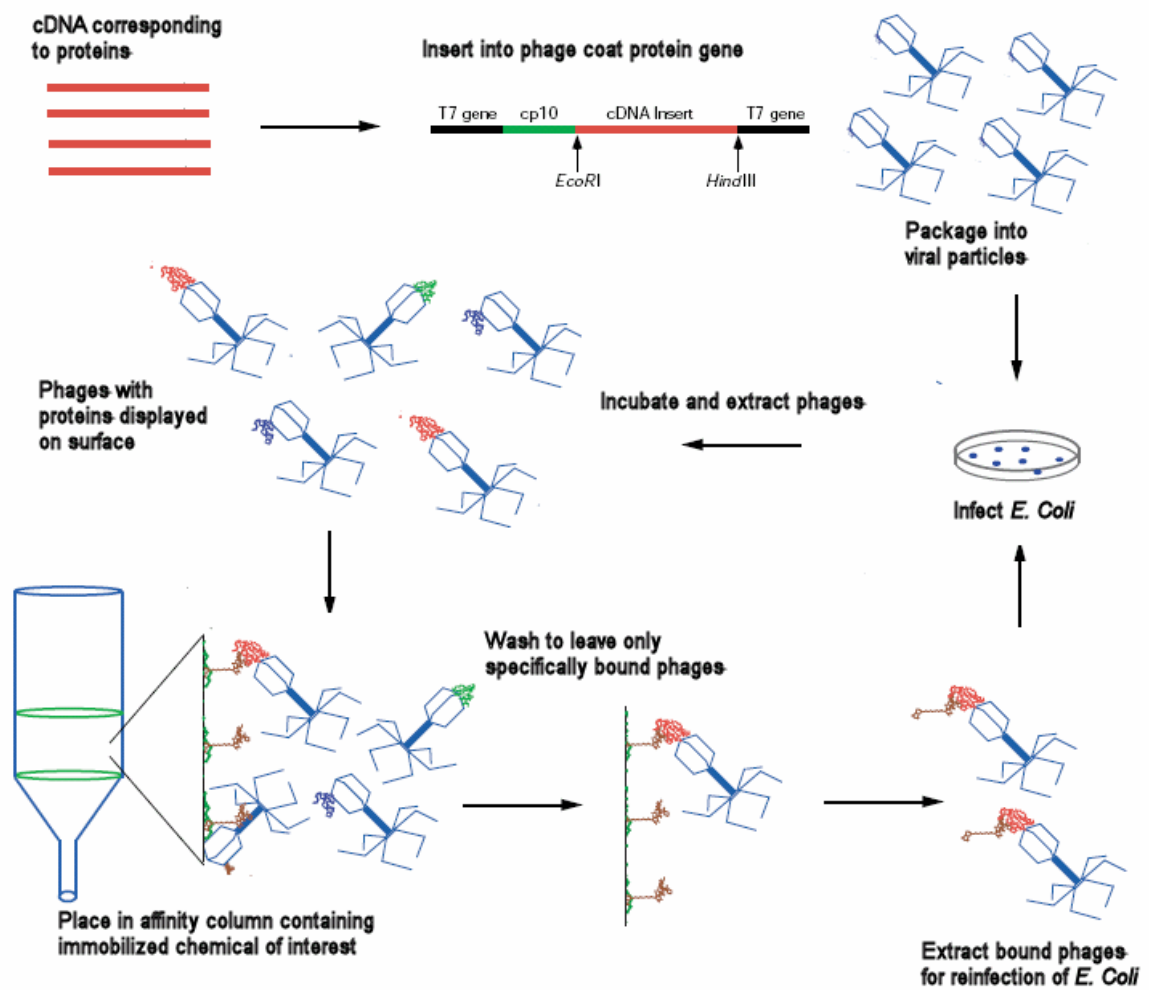


Figure 2: A schematic diagram demonstrating the principles of phage display. First, cDNA of the proteins required to display on the bacteriophages is collected. These are inserted into many copies of the phage coat gene altogether and packaged into viral particles. These are incubated in *E. coli* to produce phages that display the required proteins on their coats. Affinity chromatography is performed on a surface with immobilized small molecules, in which the phages are washed to leave only those which have bound to the column specifically. These phages are reinfected into *E. coli* to amplify them. After several rounds, the proteins found are identified by analysing the phage coat gene insert. Images from (Sche, McKenzie et al. 1999)

At Warwick HRI, the MagicTag™ system has been used to investigate the interaction of proteins from *Arabidopsis thaliana* in the immobilisation of small plant hormones such as indole acetic acid (IAA) and abscisic acid (ABA) and other molecules including glutathione (GSH), for the usage of phage display techniques.

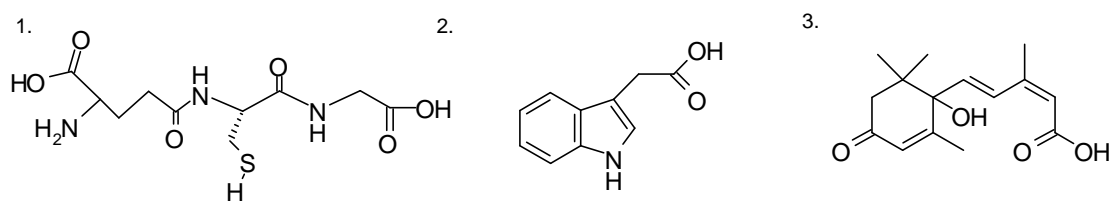


Figure 3: Molecular structures of the small molecules used in this study: (1) Glutathione (GSH), (2) Indole acetic acid (IAA), (3) Abscisic acid (ABA)

Glutathione is a tripeptide (Fig. 3.1) which occurs as an antioxidant in all plant cells (Heldt), and is also considered to be the major storage and transport compound of sulphur in plants (Dey and Harbourne). IAA (Fig. 3.2), proverbially known as auxin, is a hormone that causes cell elongation at the tips of growing shoots, and ABA (Fig. 3.3) is the hormone that causes the stomata of leaves to close during water shortages and maintains the dormancy of seeds and buds by affecting gene expression. Although ABA was discovered in the 1960s, no known receptor has been found even though the physical effects of ABA on stomata are well known.

As the binding of the protein to the immobilised hormone is specific, there is a need to find the most likely orientations of the of the hormone with respect to the surface, by finding the parts of the molecule the photoreactive groups of the MagicTag™ system attach to.

The aim of this study is to characterise the modes of attachment of GSH, IAA and ABA to a silica bead-supported phenyl azide and trifluoromethyldiazirine which comprise part of the photoreactive tags used in the MagicTag™ system using solid-state ^{13}C nuclear magnetic spectroscopy and infrared spectroscopy.

As a complementary technique to NMR spectroscopy, infrared (IR) spectroscopy was performed on all the samples (Bellamy 1995), where the transmittance of a range of frequencies of infrared light is measured. The transmittance of the light of the samples depends on the frequency of absorbance of light by the electrons in bending and stretching covalent bonds, and so the nature of bonds in the sample can be elucidated. This method does not give such specific structural information as NMR spectroscopy.

Basics of NMR Spectroscopy

Nuclear magnetic resonance is a spectroscopic technique in which the frequency of precession of nonzero-spin nuclei (such as ^1H and ^{13}C) in a strong magnetic field of a sample is detected. The frequency of this precession (the Larmor frequency) is proportional to the strength of the magnetic field, but depending on the microscopic magnetic environment of a nucleus (affected by the surrounding electrons and nuclei) the precession frequency of the nucleus can change very slightly, giving highly localised information about the nucleus' chemical environment.

Subatomic particles such as quarks (which make up nuclei) and electrons have an intrinsic angular momentum different to the macroscopic sense known as spin, which generates a magnetic moment associated with the particles from the spinning of the charged particles. The moment could be in the same or opposite direction to the spin axis. Nuclei such as ^1H (proton) and ^{13}C have spin $\frac{1}{2}$, and have their magnetic moment in the same direction as their spin, whilst the most common carbon isotope, ^{12}C , has no spin and does not generate a magnetic moment. In a sample in equilibrium in the absence of an external magnetic field the distribution of magnetic moments is isotropic.

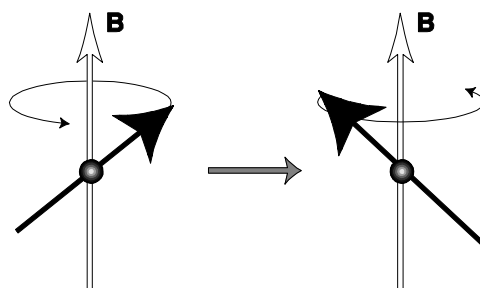


Figure 4: Spin precession of (positive-spin) nuclei in a magnetic field, B. The frequency of this spin is known as the Larmor frequency of the nucleus (Levitt 2003).

When a magnetic field is suddenly applied to the sample, the net magnetic moment of the nuclei slowly builds up in the direction of the field, but this is only very slight: in protons at room temperature only 10001 against 10000 spins are aligned towards the field rather than in the opposite direction. Instead of the nuclear spins aligning towards the field as in a compass towards a bar magnet, the axes of the spins precess in the direction of the field (Fig. 4) at the

Larmor frequency $\omega^0 = -\gamma B^0$, analogous to a spinning top (the ‘spinning’ nucleus) with a tilted axis acting against gravity (the external magnetic field). In an 11.7T magnet, ^1H precess at around 300MHz whilst ^{13}C precess at 75.4MHz.

The build-up of net nuclear magnetic moment, or longitudinal magnetic moment, is known as the longitudinal relaxation time and is denoted T_1 , which can range from ms to years depending on the physical properties of the sample, and the state reached is known as thermal equilibrium (Fig. 5). These precessing magnetic nuclei do generate an electric current, but the change in the longitudinal magnetism is minute compared to the electronic magnetism and is undetectable.

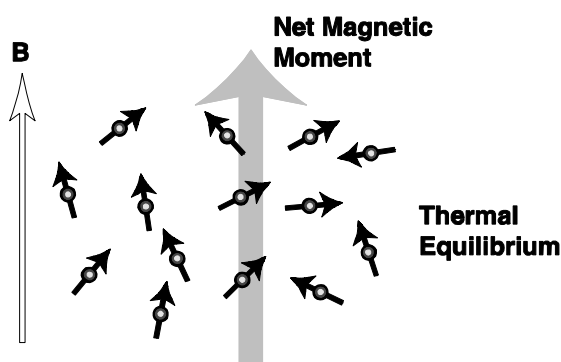


Figure 5: Thermal equilibrium. The net magnetic moment is parallel to the magnetic field (Levitt 2003).

In NMR spectroscopy, instead of measuring the longitudinal magnetisation, the spins of the nuclei are rotated by $\pi/2$ (to the $-y$ axis, for example) by an appropriate radiofrequency pulse, which changes the net magnetic moment to the $-y$ axis (Fig. 6).

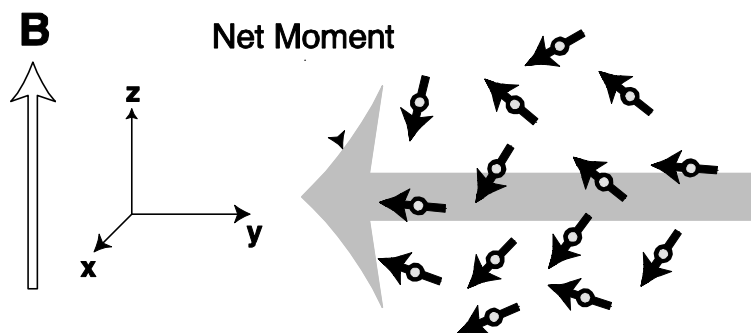


Figure 6: The net magnetic moment after application of a radiofrequency pulse (Levitt 2003).

After the pulse, the nuclei precess around the magnetic field as normal, but now the net magnetic moment changes from the $-y$ axis to the $-x$ axis etc. (in a clockwise direction for nuclei with positive γ). The changing transverse magnetisation of the sample is detected by a sensitive coil (Fig. 7), which generates a sinusoidal electric current known as the NMR signal or free-induction decay (FID), and is analysed by Fourier transform methods to extract the Larmor frequencies of the nuclei.

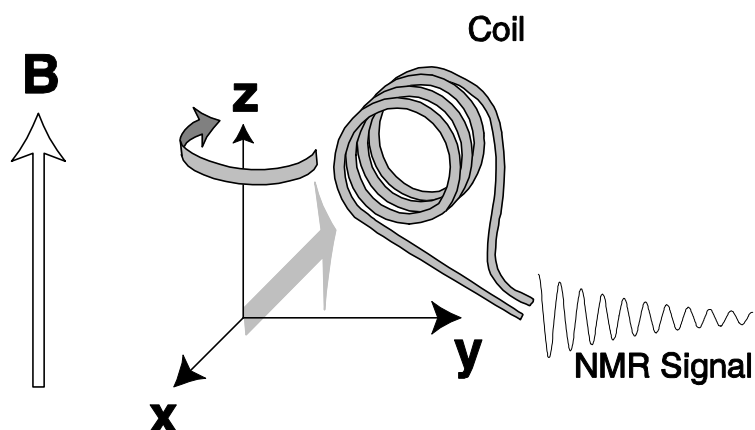


Figure 7: The changing transverse magnetisation induces an electric current in a coil, which is the NMR signal.

This spectroscopic technique gives information on a submolecular scale to a high resolution as electrons and other nuclei around the atoms of interest subject the nuclei to slightly different magnetic fields, hence their precessions are at different rates. To quantify this change in precession rate, the chemical shift is defined as the relative difference in Larmor frequency of the NMR peaks ω^0 to a reference compound ω^0_{TMS} (TMS – tetramethylsilane for ^1H and ^{13}C spectra), with units parts per million (ppm).

$$\text{Chemical shift: } \delta = \frac{\omega^0 - \omega^0_{TMS}}{\omega^0_{TMS}}$$

As the nuclei are precessing at slightly different rates, after several milliseconds to a few seconds, the FID decays as the spins become out of synchronisation with each other and the net transverse magnetisation decreases, hence loss of signal. The time elapsed for this is known as the transverse relaxation time (denoted T_2), but the experiment cannot be performed again until the longitudinal magnetism has built up again (in time T_1).

¹³C CP MAS Solid-State NMR Spectroscopy (¹H decoupled)

¹³C NMR spectroscopy is a powerful technique in finding the modes of attachment of the small plant hormones to the photoreacted solid supports as it is very sensitive to the different chemical environments of the ¹³C in the molecule, which in organic chemistry there are many. If a carbon in a molecule becomes bonded to an electron-withdrawing group such as a peptide bond after a reaction, its chemical shift will noticeably change and easily detected by NMR.

MAS

As the experiments involve attaching plant hormones to solid silica beads, then solid-state NMR is inevitably used. Solids and powders are crystalline to some extent, and the chemical shift of each crystal depends on the orientation of them with respect to the magnetic field (chemical shift anisotropy), giving undesirable broad spectra corresponding to each possible crystal orientation.

In magic angle spinning (MAS) methods, the problem is solved by spinning the whole sample in a special rotor at 54.74° (the magic angle), which drastically reduces the effects of chemical shift anisotropy and direct dipole-dipole couplings (the magnetisation of nuclear spins through space unmediated by electrons), reducing the line-widths and increasing the heights of spectral peaks, giving similar spiky spectra as liquid-state NMR.

¹H Decoupling

In 'normal' ¹³C NMR experiments, spectral peaks have a fine multiplet structure (known as J-splitting) due to the immediately surrounding magnetic nuclei (usually ¹H) engaging in indirect dipole-dipole coupling (or J-coupling) in which the magnetic field of the carbons are affected by the electronic magnetism caused by the neighbouring ¹H nuclei.

Although J-coupling caused by protons is useful in many applications, it was undesirable in this application as it causes signal intensity to be distributed over several peaks and cause the relatively broad peaks of solid state NMR to be even broader, and also the extra peaks would make the spectrum more difficult to interpret, as the sample is dilute in the carbon chemicals

which were required to be analysed (most of the sample is silica) which would give more noise.

To eliminate $^{13}\text{C} - ^1\text{H}$ J-splitting in the experiment, radiofrequency pulses are applied at the ^1H Larmor frequency to decouple the proton spins whilst the FID of the ^{13}C nuclei was being detected. This is known as heteronuclear decoupling (Fig. 8). Modern decoupling pulse schemes such as two-particle phase modulation (TPPM) are commonly used, and are usually implemented after a cross-polarization pulse (Fig. 9).

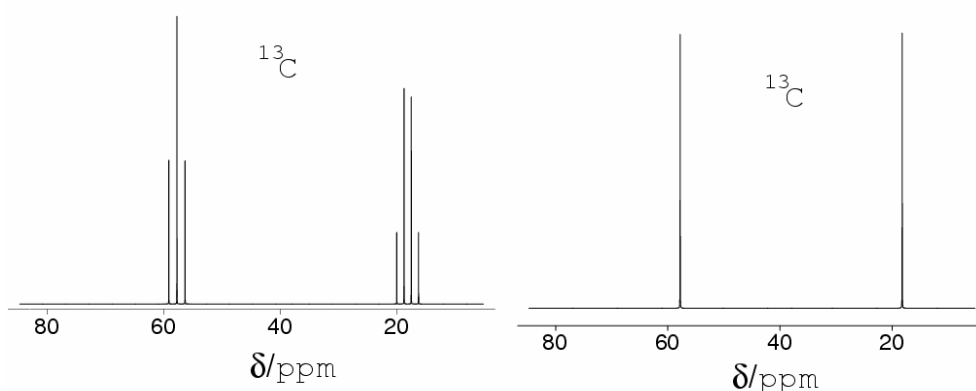


Figure 8: The ^{13}C solution-state NMR spectrum of ethanol (left) without heteronuclear decoupling, displaying multiplet structure, and (right) heteronuclear decoupled, with one sharp peak corresponding to chemically-distinct carbons (Levitt 2003).

Cross-polarization (CP)

In general, nuclear isotopes with higher magnetogyric ratios (such as ^1H) are easier to observe than those with lower magnetogyric ratios (such as ^{13}C), as they are polarised more greatly by an external magnetic field (giving a stronger signal) and return to thermal equilibrium faster: T_1 is several times shorter for ^1H nuclei than for ^{13}C - experiments can be repeated with less delay. Also, protons are much more abundant than ^{13}C , hence giving a stronger signal.

The polarisation of spin in the ^1H nuclei can be transferred to ^{13}C nuclei by applying an appropriate simultaneous pulse on both the ^1H and ^{13}C Larmor frequencies; this is known as the nuclear Overhauser effect (NOE). This transfers the above desirable properties above to the ^{13}C nuclei - giving a stronger signal than if the ^{13}C were magnetised on their own as ^{13}C is not very abundant, and increasing the number of repetitions of the experiment within a

timeframe, increasing the signal-to-noise ratio. A disadvantage is that the peak heights of the resulting spectrum are no longer quantitative of the proportions in the sample.

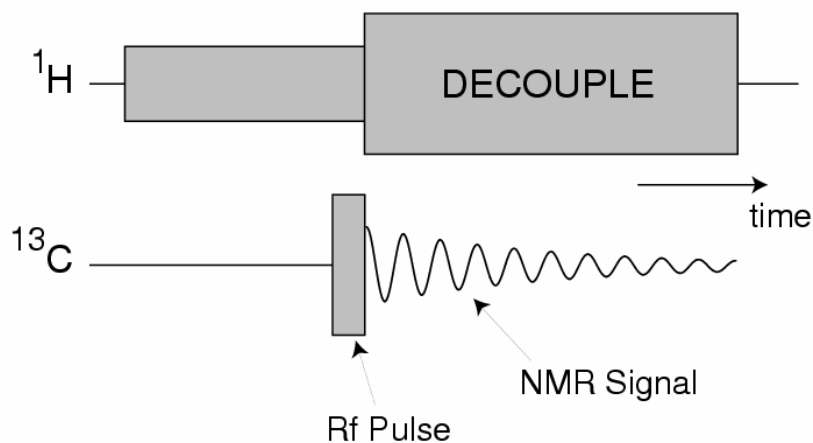


Figure 9: A simple pulse scheme implementing cross-polarisation and heteronuclear decoupling in ^{13}C NMR. A radiofrequency pulse is applied to rotate all ^1H spins 90° , which rotates the direction of the net magnetic moment from parallel to the field by 90° . This magnetisation is transferred to the ^{13}C nuclei by means of an appropriate simultaneous pulse on both the ^1H and ^{13}C frequencies (cross-polarisation), followed by a decoupling pulse to reduce the influence of the ^1H spins whilst the ^{13}C signal is recording (Levitt 2003).

The chemistry of the photoreactive tags

Two of the tags of the MagicTag™ system have a phenyl azide (Fig. 10) and a diazirine group (Fig. 13), which are photoreactive groups commonly used in photoaffinity labelling (Fleming 1995): the placement of a photoreactive group on either the enzyme or substrate and exposing the complex formed to light, causing a covalent bond to form between them. The resulting enzyme-substrate can be analysed by a various methods to extract information such as the position of the binding site and kinetics of the reaction.

In MagicTag™, the photoreactive groups are used to immobilize ligands covalently. When the azide group in phenyl azide is exposed to ultraviolet light (254nm), nitrogen gas is released and a reactive species known as a nitrene is produced (Figure 1).

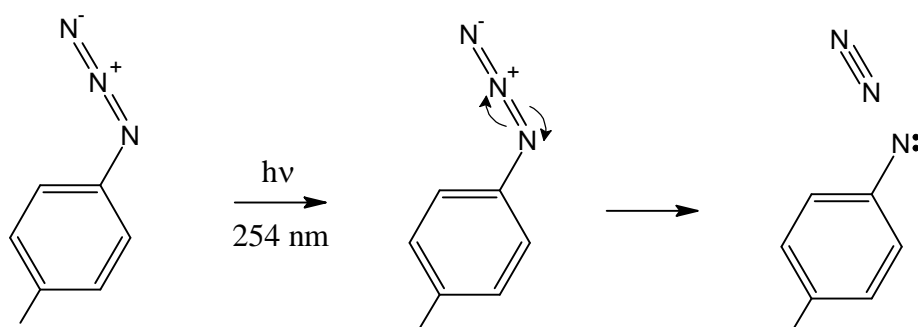


Figure 10: The mechanism of photolysis of a phenyl azide under ultraviolet light. The N=N bonds in the azide (left) become excited under radiation, and a phenyl nitrene and nitrogen gas is formed (right).

Nitrenes are an extremely reactive species in which the nitrogen only has six electrons on its outer shell, hence two unshared pairs of electrons, and can exist in two different electronic states with differing properties – singlet and triplet. In aryl nitrenes, the ground state is usually the singlet state (as the two lone pairs in the singlet is delocalised by the benzene ring), but the enthalpy change from singlet to triplet is only 3 kcal/mol, which means it usually exists in both states at room temperature.

In this study, a silica-bead supported phenyl azide with a thiourea group (Fig 11.1) was used – although the chemical properties of the benzene ring change slightly depending on the nature of the groups attached, the nitrene produced should have similar properties to the PEG chain

phenyl azide used in the MagicTag™. A silica azide with a peptide bond (Fig.11.2) was also used in one experiment.

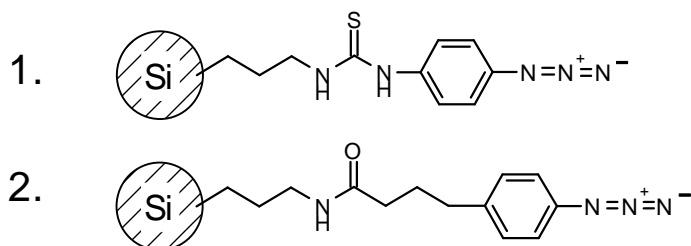


Figure 11: Structures of the silica bead-supported phenyl azides used in this study: (1) thiourea silica azide and (2) peptide silica azide.

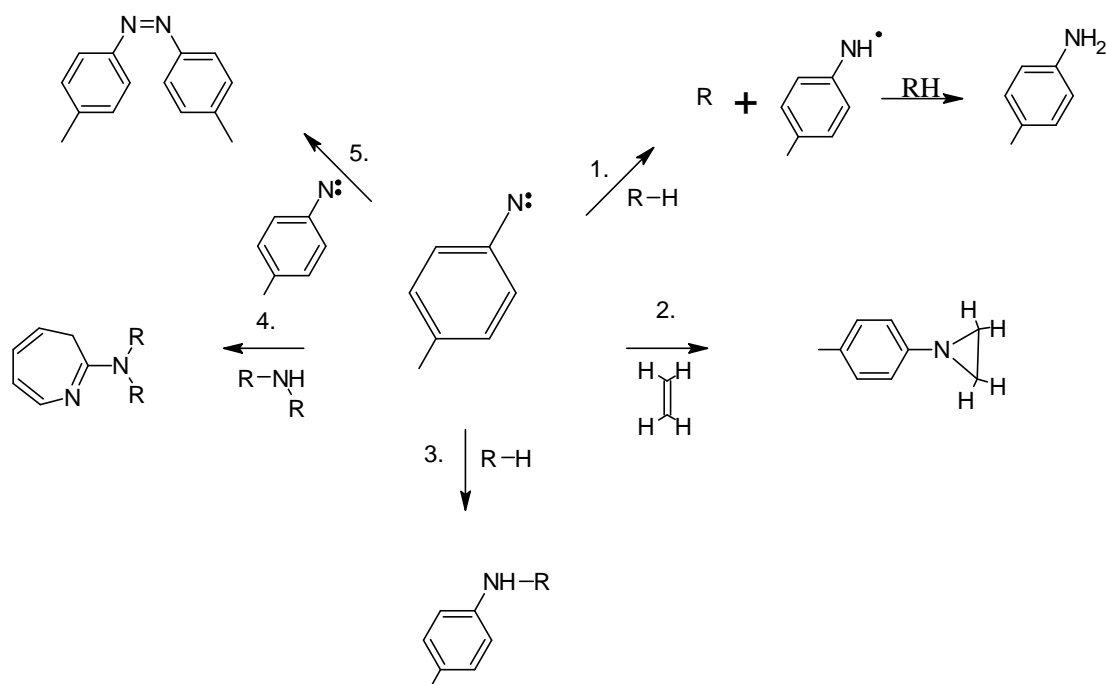


Figure 12: Some typical reactions of aryl nitrenes. (1) is the abstraction of hydrogen, where hydrogen is removed from hydrocarbons by the nitrene to form a primary amine. (2) is insertion into a multiple carbon bond; (3) insertion into a carbon bond, probably the most desirable reaction for tagging molecules; (4) ring expansion caused by a suitable nucleophile and (5) is dimerization with another nitrene (Lwowski 1970).

The other photoreactive ligand used in this study is SJD-IV-707, silica bead-supported trifluoroethyldiaziriny benzene (a diazirine group containing compound) as used in MagicTag™ (Fig. 13).

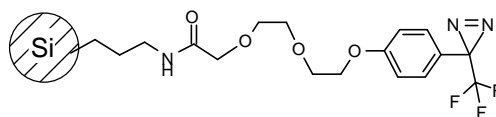


Figure 13: SJD-IV-707, a ligand used in the MagicTag™ system, with the diazirine photoreactive group on the top right.

When the diazirine ligand is exposed to visible light, nitrogen gas is also produced, but the reactive intermediate is a carbene, an electron-deficient carbon. The diazirine tag has a trifluoromethyl group bonded to the carbene carbon; this is an electron-withdrawing group that helps to stabilize the lone electron clouds of the carbene to stabilize its singlet spin state.

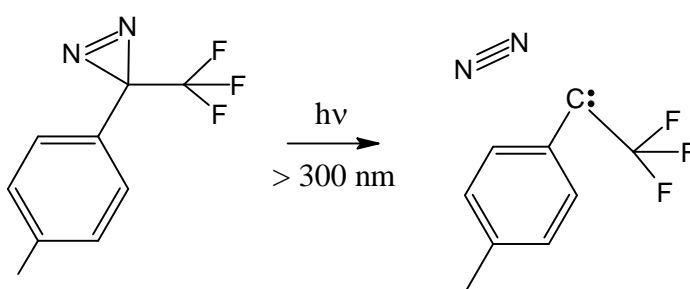


Figure 14: The photolysis of a phenyl diazirine under visible light. It will sometimes interconvert to a diazo group, which has a similar photochemistry to the diazirine (Fleming 1995).

The carbene undergoes similar reactions to nitrenes, but dimerization of the nitrenes as in Fig. 12.5 occurs less often and ring expansion as in Fig. 12.4 is not evident in aryl carbenes, hence they are probably a more reliable photoreactive species than the aryl nitrenes (Platz 1995). Also, nitrogen bonds may be easily photolysed compared to carbon bonds, and as the azide is activated in the ultraviolet range, the radiation may destroy or alter some biological molecules (Fleming 1995).

However, the nitrene has modes of chemical reactions not open to the carbene, for example carbene reactions with amines form a C-N bond which is reversible unlike the nitrene. Also, the diazirine used can react with molecular oxygen and is very sensitive to ambient light (Fleming 1995).

Materials and Methods

The photoactive supported tags were supplied by Suzanne Dilly, which were manufactured using propylamino silica beads - derivatised silica beads with amino (NH₂) groups attached. For example, the thiourea silica azide was manufactured from the reaction of propylamino silica (Acros Organics, concentration of amino group 1.4mmol/g) and 4-Azidophenylisothiocyanate (Sigma-Aldrich) (Fig. 15).

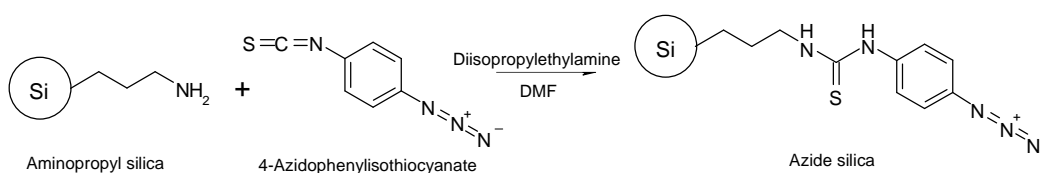


Figure 15: Reaction scheme of the preparation of the thiourea silica.

As much of the molecular weight of the photoactive tags are silica, it is not useful to talk about its molar weight, but in terms of the concentration of active functional groups attached to the silica known as the loading concentration.

Table 1: Summary of the samples prepared.

Sample number	Sample name
1	SJD-IV-707 + glutathione + water
2	SJD-IV-707 (unreacted)
3	Thiourea silica azide
4	Thiourea silica azide + glutathione + water
5	Thiourea silica azide + IAA + water
6	Thiourea silica azide + IAA + DMSO
7	Thiourea silica azide + ABA + water + 20 drops DMSO
8	Peptide silica azide + glutathione + water
9	Thiourea silica azide + water

Sample 1

A solution of glutathione (Lancaster, 53mg, 0.172mmol) in water (1ml) was added to a dark sample of SJD-IV-707 (60mg, loading conc. 0.96mmol/g) and revealed to light for 23h. The cap of the reaction vial was perforated to release excess nitrogen gas caused by the reaction.

The product was then washed 5 times with water, methanol and acetone respectively to wash away any excess glutathione which had not bound to the silica (using a gel filtration column under a partial vacuum), then left to dry for approximately 1.5h in the column, which yielded

40mg of dry product for infrared spectroscopy (immediately) and solid-state NMR spectroscopy (within 24h).

Sample 2

An unreacted sample of ~60mg of SJD-IV-707.

(This was packed into a Bruker 4mm NMR rotor in the dark, and placed into the probe immediately to minimise exposure to light.)

Sample 3

A unreacted sample of thiourea silica azide (60mg, loading conc. 1.12mmol/g).

Samples 4-7

For each of these experiments, the solution added and weights of the thiourea silica azide used and the dry product obtained are given in Table.

1ml of solution was added to ~70mg of thiourea silica azide (loading conc. 1.4mmol/g) and exposed to ultraviolet light (254nm) for ~23h. The caps of the reaction vials were perforated to release excess nitrogen gas caused by the reaction. The product was then washed 5 times (with water, methanol and acetone respectively) as in the preparation of sample 1 with the same apparatus, then left to dry for approximately 1h.

Table 2: Details of the solutions used, mass of silica azide used and mass of dry product obtained in the preparation of samples 4-7 for infrared and solid-state NMR spectroscopy.

Sample	Solution		Silica azide used (mg)	Dried product obtained after reaction (mg)
	Solute	Solvent		
4	Glutathione (Lancaster, 53mg, 0.172 mmol)	Water (1ml)	71	55
5	IAA (Lancaster, 30mg, 0.171 mmol)	Water (1ml)	70	51
6	IAA (Lancaster, 30mg, 0.171 mol)	DMSO (1ml)	70	56
7	ABA (Sichuan Lomon Bio technologies Co. Ltd., China, 31mg, 0.117 mmol)	Water (0.8ml) + DMSO (20 drops)	70	55

Sample 8

This sample was prepared similarly to sample 4, but instead of using thiourea silica, the newly synthesised peptide silica azide, in which the thiourea bond is replaced by propylamido bond.

To test the effectiveness of this photoreactive tag, it was reacted with glutathione as in sample 4, in which gave was a high proportion of binding.

A solution of glutathione (Lancaster, 53mg, 0.172 mmol) in 1ml water, was added to ~70mg of peptide silica azide (loading conc. 1.11mmol/g), and exposed to ultraviolet light (254nm) for ~23h. The caps of the reaction vials were perforated to release excess nitrogen gas caused by the reaction. The product was then washed 5 times (with water, methanol and acetone respectively) as in the preparation of sample 1 with the same apparatus, then left to dry for approximately 1h.

Sample 9

1ml of water was added to 70mg of thiourea silica azide (loading conc. 1.4mmol/g) and exposed to ultraviolet light (254nm) for ~23h. The caps of the reaction vials were perforated to release excess nitrogen gas caused by the reaction. The product was then washed 5 times (with water, methanol and acetone respectively) as in the preparation of sample 1 with the same apparatus, then left to dry for approximately 1h.

Infrared Spectroscopy

The infrared spectroscopy was performed on an Avatar 320 FTIR (Thermo/Nicolet Instrument Corporation) operating in ATR mode. The spectrometer was run using the software EZ-OMNIC 5.0 (Thermo/Nicolet Instrument Corporation). The germanium crystal was cleaned and a background spectrum was run. A few grains of siliceous sample were placed on the crystal, the gate and clamp lowered onto the sample, and the spectrum was recorded (wavelengths from 4000cm^{-1} to 450cm^{-1} wavenumbers), compared with the subtracted background, and converted into percentage transmittance.

Solid-State MAS NMR spectroscopy

The NMR spectroscopy was performed on a 300MHz spectrometer (7.05 Tesla) using the Chemagnetics data acquisition system (CMX Infinity, Chemagnetics, For Collins, USA), and operated by the Varian Infinity Plus spectrometer (Varian Associates Inc., Palo Alto, USA) and using the software Spinsight (Version 4.1, Varian Associates Inc., Palo Alto, USA). All samples were loaded into a 4mm rotor with standard packing tools and placed inside a 4mm

probe. The rotors and packing equipment were cleaned with isopropanol (propan-2-ol) beforehand. The probe was tuned at the frequencies 300.1MHz for ^1H and 75.5MHz for ^{13}C initially using a network analyser (RF Network Analyser, No. 8712RET, Agilent Technologies Inc. Palo Alto, USA) and then by an oscilloscope (Tektronic 244SB 200MHz). The shim magnets were tuned for the particular probe before probe insertion. The forward to reflected power ratios for ^1H was about 40 and for ^{13}C was no less than 4. The calibration of optimal ^1H 90 pulse length and chemical shift was performed on an L-Alanine sample rotating at 8kHz. Results were obtained using a ramped cross-polarisation method with TPPM decoupling, and the NMR spectrum for each sample was a sum of 19000-25000 distinct acquisitions, taken over the course of 18 - 23 hours.

^{13}C NMR prediction

The predictions of ^{13}C NMR peaks were performed on the ChemDraw Ultra® chemical drawing package, part of the ChemOffice 7 (CambridgeSoft, Cambridge, MA, USA) software package.

Results and Discussion

Sample 1 - SJD-IV-707 + glutathione + water

From the progress of the reaction and IR spectrum (Appendix Fig. 2) of the sample, there was nothing unusual as nitrogen gas was released throughout the reaction and the glutathione appeared to attach from the IR spectrum, but in the solid-state ^{13}C NMR spectrum (Appendix Fig. 3), there were only very small peaks in the 110-150 ppm range (Fig. 16) corresponding to aromatic carbons, which would correspond to the benzene group (being the only aromatic carbons present) in the SJD-IV-707. The NMR spectrum implied there was very little intact SJD-IV-707, either because of the nature of the reaction or problems with the sample of SJD-IV-707.

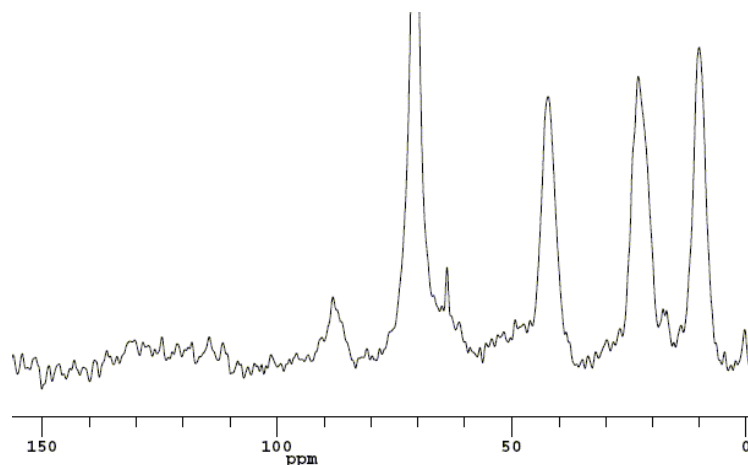


Figure 16: The ^{13}C solid-state NMR spectrum of the SJD-IV-707 + glutathione + water spectrum (0 – 150 ppm), demonstrating the lack of peaks at the 100 – 150 ppm range, which should correspond to the benzene carbons in SJD-IV-707.

Sample 2 - SJD-IV-707 (unreacted)

The SJD-IV-707 was packed in a MAS NMR rotor in the dark (courtesy of S. Brown), and the solid-state NMR spectrum recorded. As in the sample 1 spectrum, there were only very small peaks in the 110-150 ppm range (Fig. 17), indicating there were hardly any aromatic carbons (i.e. benzene carbons) in the SJD-IV-707 sample, hence the sample used had no phenyl groups.

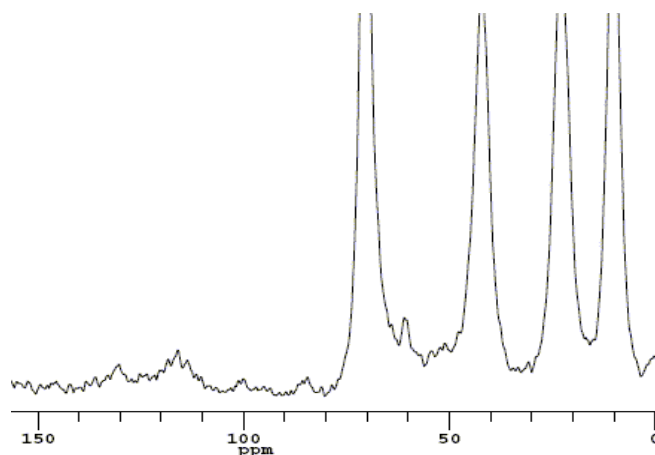


Figure 17: The ^{13}C solid-state NMR spectrum of the SJD-IV-707 (0 – 150 ppm, full spectrum (Appendix Fig. 4)), demonstrating the lack of peaks at the 100 – 150 ppm range, which should correspond to the benzene carbons in SJD-IV-707.

Sample 3 – Thiourea silica azide (unreacted)

From the disappointing conclusions of the last two samples, the attention was turned onto the azide silica sample. The IR spectrum (Appendix Fig. 5) showed a peak at 2119nm corresponding to an intact N_3 (azide) peak, but to check the structure of the molecule, solid-state NMR was performed on the sample (Appendix Fig. 6), and from the three peaks in the 110 – 150 ppm region, a benzene ring was present (Fig. 18).

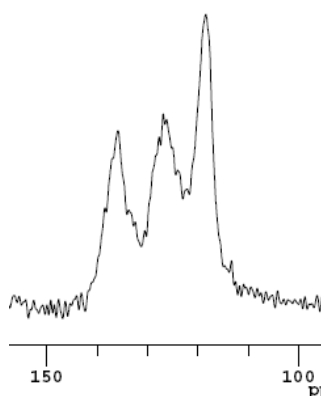


Figure 18: The 100-150ppm region of the ^{13}C solid-state NMR spectrum of thiourea silica azide, showing strong peaks in this region indicating the presence of a benzene ring in the sample.

In total, there were 8 distinct peaks of the ^{13}C spectrum, and 8 different chemical environments for the carbons in thiourea silica azide. To assist in assigning peaks to parts of

the molecule, the ^{13}C NMR predictor in ChemDraw was used, although it predicted carbon shifts of attached azide groups incorrectly.

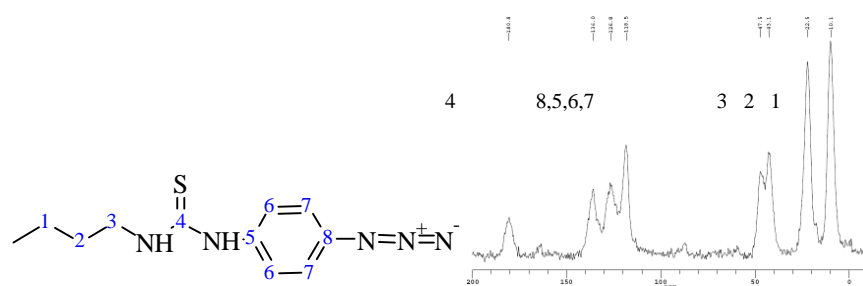


Figure 19: Numbered chemically-equivalent carbons in the thiourea silica azide molecule, and approximate allocation of NMR peaks to the thiourea carbons.

The thiourea carbon, 4, has a shift of 180.8, whilst 1, 2 and 3 correspond to the three or four peaks less than 48 ppm. The phenyl carbons (5, 6, 7 and 8) must correspond to the three peaks 136.0, 126.8 and 118.5 although there may be smaller peaks in this region obscured by the broad peaks.

Sample 4 – Thiourea silica azide + glutathione + water

The IR spectrum of the sample (Appendix Fig. 7) showed the N_3 peak had completely disappeared; hence the azide group had almost completely reacted. There were also a new peak at 1627 cm^{-1} (peptide bond) and a broad region of absorbance at the $3700 - 2700\text{ cm}^{-1}$ range compared to sample 3, which correspond to the attachment of glutathione.

When ^{13}C solid-state NMR was performed on the sample, the results confirm there was notable attachment to glutathione, as peaks appeared on the spectrum (Appendix Fig. 8) which correspond to a solution-state ^{13}C NMR spectrum of glutathione in D_2O (Fig. 20) such as the 173.6 (amide group) and 54.0 ppm peaks.

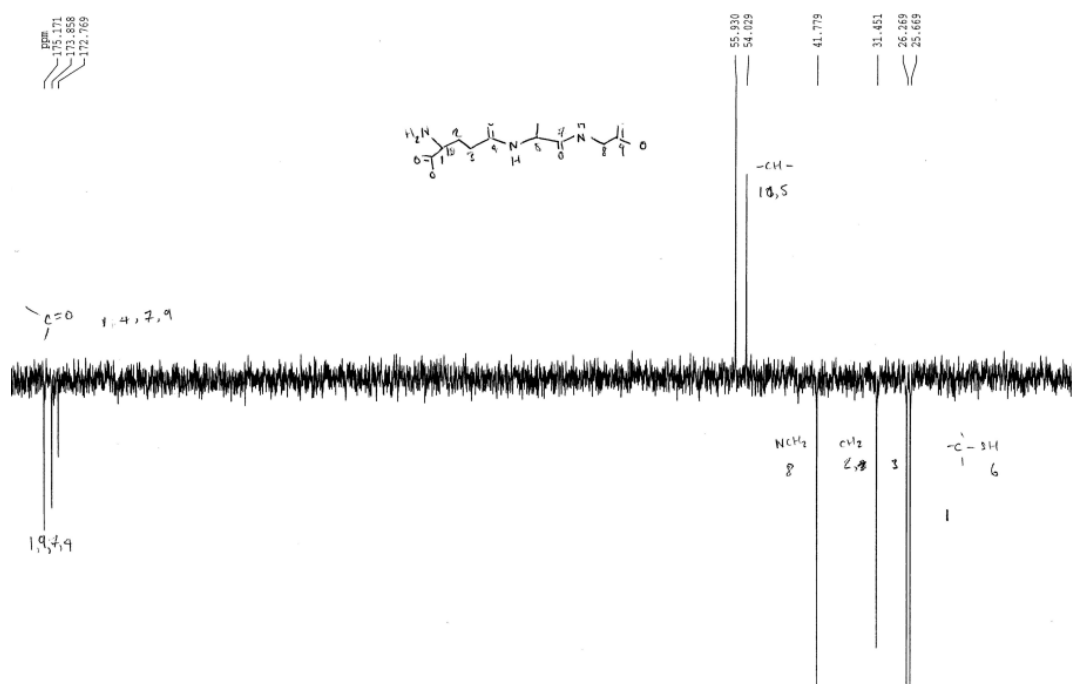


Figure 20: Solution-state NMR of glutathione dissolved in D₂O, using a Bruker DPX300 spectrometer with 300MHz magnet. Note there are no peaks in the 100 – 150 ppm region. The peaks are numbered with the probable carbon corresponding to the small diagram of glutathione.

The most useful area of the spectrum to study was the phenyl (100 – 150ppm) region, as the chemical environment change in the azide would be sensed by the nearby carbons, and also because the spectrum of glutathione does not contain any peaks in this region due to its lack of phenyl groups. Consequently, a large change had happened to the chemical shifts in this region, which suggest other groups had replaced azide in the reaction.

To help with finding the possible attachments of glutathione to the silica azide, the ChemDraw ¹³C NMR predictor was used to test different nitrogen-containing groups on the phenyl thiourea silica for suitable chemical shifts on the phenyl region (Fig. 21). The main carbon, *ortho*, *meta* and *para* carbons of the phenyl group are quite sensitive to the chemical nature of the nitrogen, hence would act like a ‘fingerprint’ for the adjoining group.

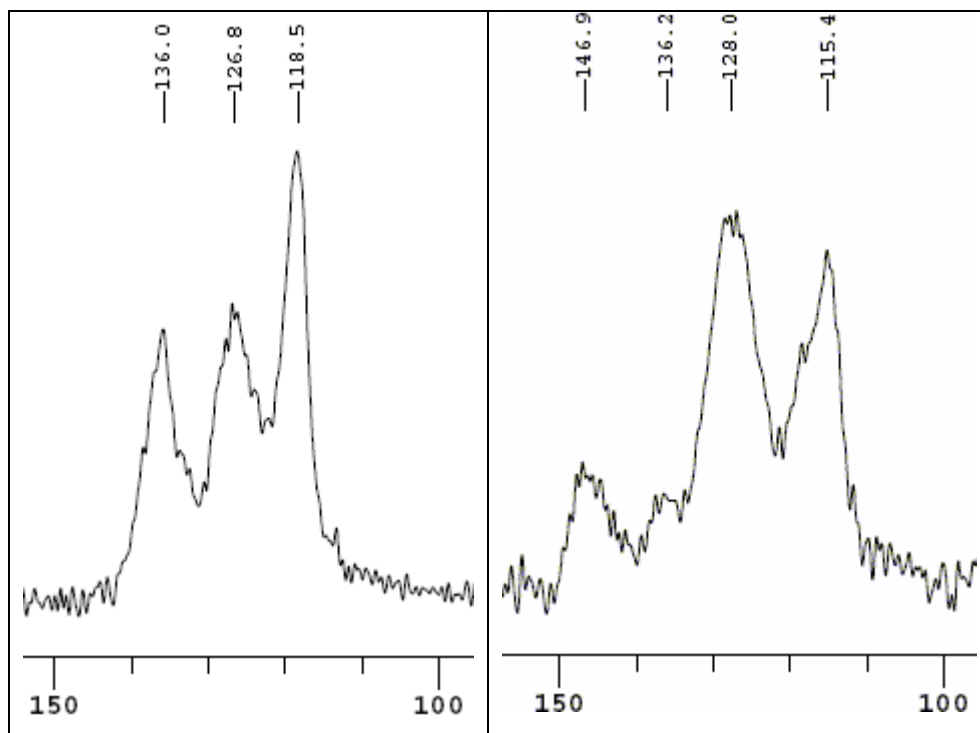


Figure 21: Comparison between the 100 – 150 ppm regions of the ^{13}C solid-state NMR spectra of unreacted thiourea silica azide (left) and thiourea silica azide + glutathione + water (right). These peaks correspond to the phenyl group, which is sensitive to the chemical nature of the former azide nitrogen. The right-hand spectrum may have been made up of many peaks, but this information was obscured by the broad peaks and noise.

The predicted shifts for the aromatic regions when attached to the $-\text{NH}_2$ group (Fig. 22.1) are 142.7, 115.4, 126.1 and 129.4, which accounts for the flat peak at 128.0 and the sharp peak at 115.4 very well, but the 142.7 shift is not consistent with the maxima at 146.9 and 136.2 hence cannot be the full characterisation, together with the fact that glutathione had certainly attached to some of the silica whilst $-\text{NH}_2$ does not involve any glutathione at all.

The reaction that would represent this product would be abstraction of hydrogen (Fig. 12.1), which is a common reaction of aryl nitrenes with hydrocarbons (Lwowski 1970). The reduction of the nitrene with glutathione was quite unsurprising, considering of its role as an antioxidant in plants.

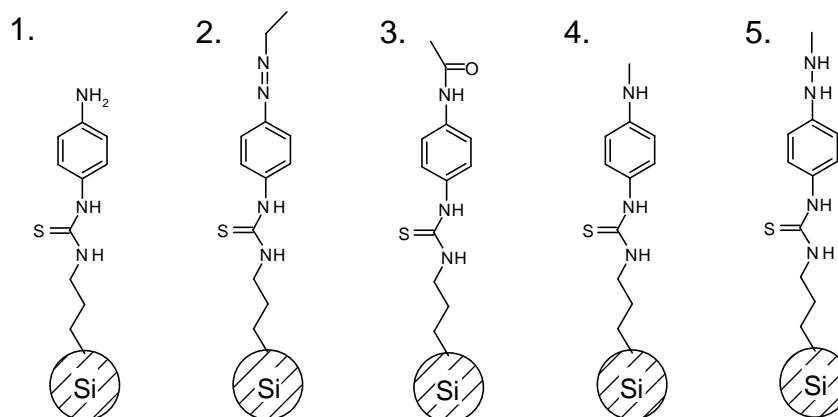
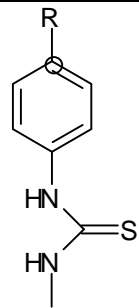
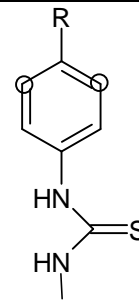
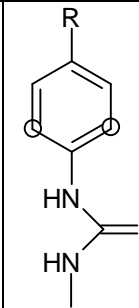
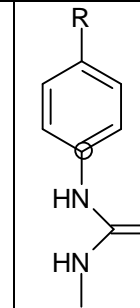


Figure 22: Probable replacements to the azide group in the thiourea silica azide + glutathione + water reaction. (1) Amino group, (2) Azo group, (3) Amido (peptide) group, (4) Secondary amino group and (5) Hydrazo group

From Table 3 of predicted ^{13}C shifts, the most likely candidate to account for the 146.9 NMR shift was the azo group of the main carbon (Fig. 22.2), whose *meta* and *para* carbon shifts are consistent with the NMR spectrum. This could correspond to the dimerization reaction (Fig. 12.5) of two nitrene radicals, but the intensity of this peak is comparable to exclusively glutathione peaks, hence is likely to correspond to insertion to glutathione as in the proposed structure (Fig. 23).

Table 3: Predicted carbon shifts (in ppm) of the phenyl carbons in the following structures, using the ^{13}C NMR predictor in ChemDraw.

R - group	 Main carbon	 <i>ortho</i>	 <i>meta</i>	 <i>para</i>
NH ₂	142.7	115.4	126.1	129.4
N=N-	146.7	122.6	125.8	136.8
NH-C=O	136.8	120.7	125.5	135.0
NHC-	139.5	112.6	126.1	127.8
NHNH-	138.2	112.3	125.8	129.8

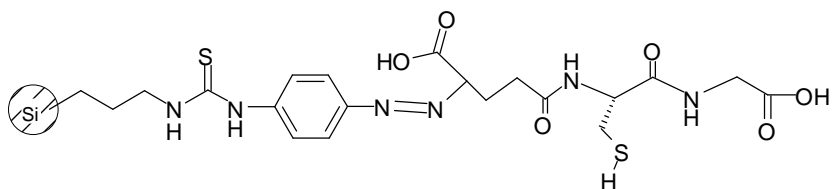


Figure 23: Proposed attachment of glutathione to thiourea silica azide via an azo bond to the N-terminus amine group of glutathione.

This result of the primary amine and the azo compound formation is consistent with free phenyl azides, which abstraction of hydrogen (from hydrocarbons, in this case the glutathione) and dimerization are two of the most common reactions (Lwowski 1970). As the azide groups are immobilized onto the silica beads and not free to interact readily with each other, the usual dimerization does not occur but instead reacts with the amino group of the glutathione.

The only peak not yet accounted for is the 136.2 ppm peak – this may correspond to unreacted silica azide, but assuming it had completely reacted from the information in the IR spectrum, this could be attributed to the formation of an amido (Fig. 22.3), secondary amino (Fig. 5.4) or the hydrazo (Fig. 22.5) bond.

The amido bond could have formed from nucleophilic attack of the aryl nitrene by the electron-rich carboxyl groups, forming a peptide bond. The hydrazo moiety is rather weak and would probably be oxidised by the energetically more favourable azo bond.

The secondary amine (Fig. 22.4) would be formed by nitrene insertion into a C-H bond (Fig. 12.3), and is a likely product due to its main carbon shift (136.8 ppm) and low *ortho* shift (112.6 ppm). Using the ^{13}C NMR predictor, the most likely carbons the nitrene would attach are the non-alpha carbons of the glutamine residue (Fig. 24), as they corresponded to predicted 'glutathione + thiourea silica nitrene' spectra without peaks in the 60 – 85 ppm region, absent in the NMR spectrum.

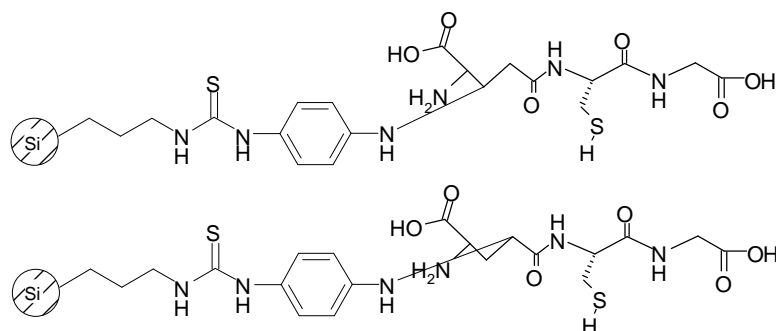


Figure 24: Two probable modes of attachment of thiourea silica azide to glutathione to produce phenyl secondary amines.

The other prominent and unusual peak in the NMR spectrum is the 87.5 ppm peak, which had subsequently appeared in all the NMR spectra of the reacted silica azides. This may be due to a reaction independent of the substances in the solution (some sort of decomposition of the product) or with the solvent water.

Sample 5 – Thiourea silica azide + IAA + water

The IR spectrum of this sample (Appendix Fig. 9) had a large peak at 2119cm^{-1} , suggesting that not much of the azide group of the photoreactive tag had reacted, hence only a very small attachment of indole acetic acid occurred. The ^{13}C solid-state NMR spectrum (Appendix Fig. 10) concurs with this, with the only major differences between this spectrum with that of unreacted silica azide is the small peak at 87.5ppm, which occurs in almost all reacted samples of the silica, and two sharp peaks at 64.2 and 25.2 ppm (SDBSWeb: <http://www.aist.go.jp/RIODB/SDBS/>) corresponding to contamination with propan-2-ol, which was used to clean the NMR rotor.

There was a small flat peak at 1610 cm^{-1} in the IR spectrum, which suggest the production of an amide bond due to the reaction of the nitrene with the carboxyl group of IAA (Fig. 25), but this insertion must be quite rare. This may have been due to the fact that the concentration of IAA was small in the solution, as it is not very soluble in water. The disadvantage of the NMR spectroscopy technique used is that it is insensitive to very small concentrations of the amide bond in this case, whose peak region was difficult to extract from the noise.

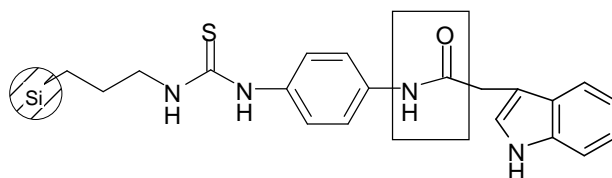


Figure 25: Proposed production of an amide bond (boxed) of thiourea silica azide with IAA.

Sample 6 – Thiourea silica azide + IAA + DMSO

To test the hypothesis that the IAA did not attach well because of its solubility in water, DMSO was tried instead, which is a better solvent for IAA. The IR spectrum (Appendix Fig. 11) of this was almost identical to sample 5, which suggests that most of the silica azide had not reacted, whilst some may have formed an amide bond with IAA, hence the concentration or solubility of IAA did not affect its reaction with the thiourea silica azide.

It was suggested that the indole acetic acid may absorb strongly at 254nm, the wavelength at which the azide becomes unstable and reactive. This hypothesis was tested by running an ultraviolet absorption spectrum of IAA (317 μ M, from stock solution of 1.03mg/ml diluted 17:1) solution in water from 350nm to 200nm (Fig. 26). The 254nm excitation wavelength was near an absorption minimum, and the extinction coefficient at this wavelength is 1577cm⁻¹mol⁻¹dm⁻³ (from $A_{254} = \epsilon_{254} cl$, where $A_{254} = 0.50$, $c = 3.17 \times 10^{-4}$ mol dm⁻³ and $l = 1$ cm) which implied that IAA has a low absorbance at this wavelength, which should not interfere with the photochemistry of the azide.

Sample 7 – Thiourea silica azide + ABA + water + 20 drops DMSO

As in sample 5 and 6, the azide N₃ peak was still present in the IR spectrum (Appendix Fig. 12), implying that only a small part of the azide had reacted. There could have been a small amount of attachment of ABA, but this would probably been obscured by the broad peaks in the solid-state NMR spectrum (Appendix Fig. 13), giving a spectrum that was virtually identical to the unreacted silica azide (except for the peak at 87.5 ppm). None of the spectroscopic techniques gave any clues to the attachment of ABA to thiourea silica azide.

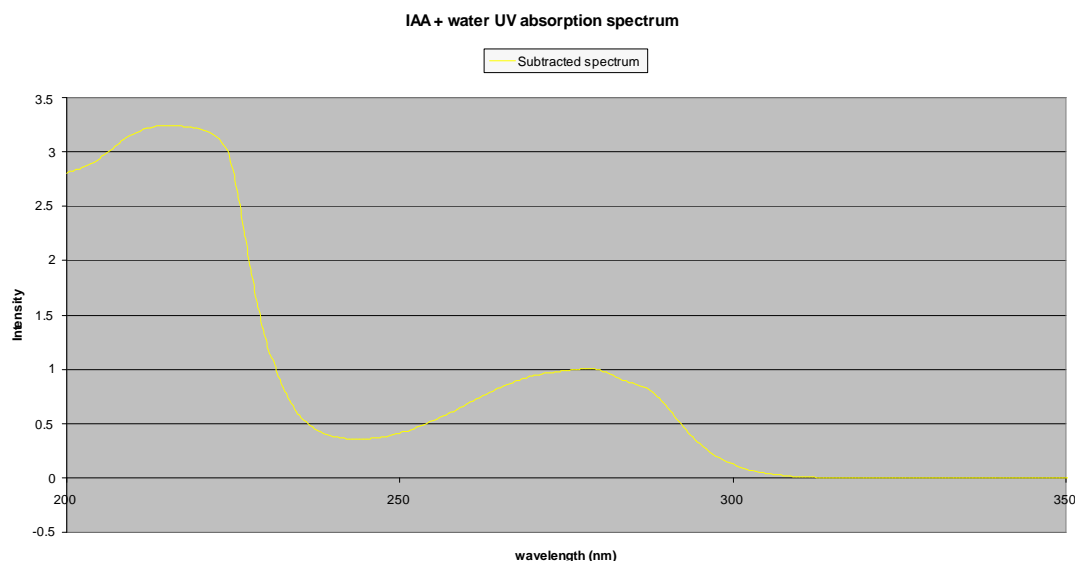


Figure 26: The UV absorbance spectrum of 317 μ M indole acetic acid (IAA) solution in water (subtracted from water spectrum). The 254nm wavelength is near an absorption minimum.

Sample 8 – Peptide silica azide + glutathione

The synthesis of this sample was the same as in sample 4, but instead peptide silica azide was used had a slightly different structure (Fig. 11.2), where the thiourea group has been replaced by a peptide (amido) bond. It was expected that each of the compounds will have similar reactivities because of the common phenyl azide groups, but there is an important difference: in thiourea silica azide, the thiourea group withdraws electrons from the benzene ring, whilst the hydrocarbon chain in the peptide silica azide is more of an electron donor.

The importance of this observation is that it may affect the reactivity of the nitrene intermediate by influencing the electron density of the benzene rings. This variation of electron density also corresponds to a change of ^{13}C chemical shifts for all the phenyl carbon nuclei, hence the ^{13}C NMR for these compounds in the 100 – 150 ppm range were expected to be quite different.

Comparing the IR spectra of the silica azides + glutathione, there seemed to be slightly less glutathione insertion (Appendix Fig. 15) than sample 4 due to the larger transmittance at the 3000 - 3500 cm^{-1} region, but the N_3 peak had disappeared as in sample 4, hence the azide had reacted.

The ^{13}C solid-state NMR spectrum (Appendix Fig. 16) was very different to the thiourea silica azide spectrum (Fig. 28) due to the sharp and large peaks in the 0 – 50 ppm region (mainly due to the aliphatic carbons in the peptide silica azide) and the large peak at 174.5ppm (due to the peptide bonds in both the azide and glutathione). This spectrum also confirms there was less glutathione insertion in the peptide silica azide than in the thiourea type from the intensity of the 54.0 ppm peak, which in both samples corresponds to the α -carbon of the cysteine residue in glutathione.

To try to find the possible products or modes of attachments of glutathione with the peptide silica azide, as in the thiourea variety, the most useful ^{13}C NMR region was 100 – 150ppm (Fig. 29). As with the thiourea silica azide, the ^{13}C NMR predictor on ChemDraw was used to give a predicted spectrum, and some probable groups replaced the azide in the peptide silica azide **Error! Reference source not found.**

The predicted chemical shifts seemed to favour the production of the $-\text{NH}_2$ group (primary amine) from the main carbon chemical shift of 144.0 close to that of the real spectral peak of 145.2, with the *ortho* (115.2), *meta* (129.1) and *para* (128.8) shifts corresponding very well to the strong NMR peaks at 115.4 and 129.4. There was a slight peak at 148.8 ppm which is likely to correspond to the azo ($\text{N}=\text{N}$) group, but this peak has much smaller prominence than in the thiourea silica azide (Fig. 6), hence is not a major product of the reaction. There was also some evidence that the amide or the $-\text{NHC}$ (secondary amino) bonds could have been formed, but this cannot be certain until the ^{13}C NMR spectrum of peptide silica azide is obtained.

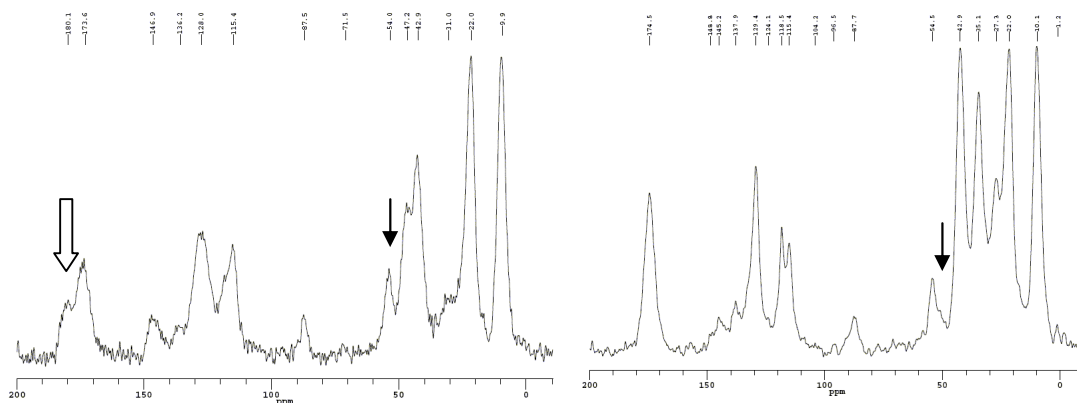


Figure 27: Comparison of the ^{13}C solid-state NMR spectra of (left) thiourea silica azide + glutathione + water and (right) peptide silica azide + glutathione + water, which has more peaks in the aliphatic region

(0 – 60ppm) and lacks the 180 ppm peak (hollow arrow) corresponding to the thiourea carbon. Note the intensity of the 54.0ppm peaks (thin arrows) corresponding to the alpha-carbon of the cysteine residue of glutathione has less intensity in right than the left spectrum, which implies there is less attachment of glutathione to the peptide variety than in the thiourea silica azide.

Comparing the conjectured main products of the thiourea silica azide with the peptide silica azide, the former produced a greater ratio of N=N: NH₂ than the latter. Although this could be a possible explanation of the lower level of attachment of glutathione of the peptide variety, the abstraction of hydrogen reaction producing the -NH₂ group has been attributed to the triplet state of the nitrene, whilst the azo-forming reactions are most likely singlet state nitrene reactions (Lwowski 1970). An explanation for this result is that the electron-withdrawing thiourea group stabilises the delocalization around the singlet nitrene, whilst the propyl group on the peptide silica azide induces the opposite effect. This phenomenon could be exploited to produce more efficiently-binding photoreactive tags.

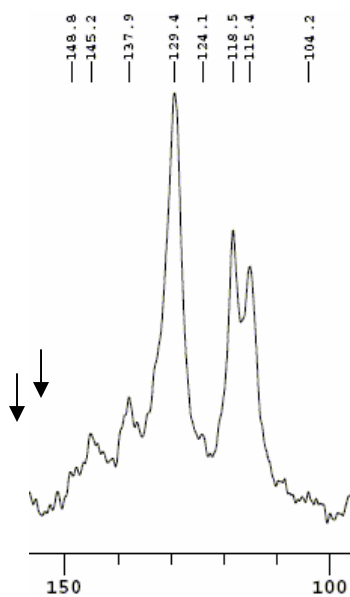
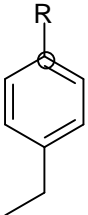
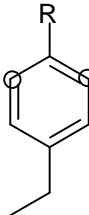
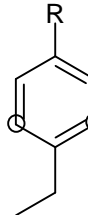
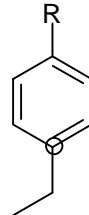


Figure 28: The 100 – 150 ppm region of the ¹³C solid-state NMR spectrum of peptide silica azide + glutathione + water. The left-hand arrow probably corresponds to the formation of the azo bond, whilst the right-hand arrow corresponds to the unattached NH₂ (primary amine) group. The other large peaks are consistent except the 137.9 ppm peak, are consistent with the proposed attached groups, although an NMR spectrum of the unreacted peptide silica azide is required to fully elucidate the peaks.

Sample 9 – Thiourea silica azide + water

This was a control sample to test whether there is an effective reaction with water of the thiourea silica azide. Also, this was used to confirm the presence of the NMR peak at 87.7ppm which appears on all the spectra of reacted thiourea and peptide silica azide.

Table 4: Predicted carbon shifts (in ppm) of the phenyl carbons in the following structures with varying R-groups based on peptide silica azide, using the ^{13}C NMR predictor in ChemDraw.

R - group	 Main carbon	 <i>ortho</i>	 <i>meta</i>	 <i>para</i>	The 211 9cm ⁻¹ 1 peak was pres ent
NH ₂	144.0	115.2	129.1	128.8	
N=N	148.0	122.4	128.8	135.8	
NHCO	138.1	120.5	128.5	134.4	
NHC-	140.8	112.4	129.1	127.2	
NHNH-	139.5	112.1	128.8	129.2	

in the IR spectrum (Appendix Fig. 17), with the same transmittance at this frequency as the unreacted thiourea silica azide, implying that the azide group had hardly reacted. This was confirmed by the NMR spectrum (Appendix Fig. 18), which was also identical, except for the larger peak at 47.7 ppm and the appearance of the 87.7 ppm peak. This peak may correspond to a by-product with water common to all of the reactions.

Both spectra suggest that the thiourea silica azide does not readily react with water (or abstract hydrogen from the water); this has large implications as chemicals could be immobilised in aqueous solutions without the silica azide reacting readily with water.

Conclusions

From the three small molecules studied to find their modes of attachment to a photoreactive silica-supported phenyl azide (thiourea silica azide), glutathione reacted most readily, from the complete disappearance of the azide peak in the infrared spectrum.

From ^{13}C solid-state NMR spectroscopy, the most apparent mode of attachment of glutathione to the thiourea silica azide was an azo bond forming at the N-terminus of the tripeptide, although a significant amount of primary amine was produced as well. There were probably a few more modes of attachment to the glutathione via insertion into a C-H bond to form a secondary amine, and reaction with a carboxyl group to form an amide, but these products were not the major products of the reaction.

The other two molecules studied, indole acetic acid and abscisic acid in water did not react with the thiourea silica azide very well at all, even when the solvent in the case of IAA was replaced by DMSO, and hence the NMR spectroscopy performed showed very little attachment of these. The absorption of IAA at 254nm, the wavelength of light the azide group is activated, was also insignificant, hence this lack of reactivity was due to other factors.

Another silica azide was prepared (peptide silica azide), which was reacted with glutathione solution as with the thiourea silica azide, and showed slightly less attachment of glutathione than the thiourea variety, which may be due to the electron-donor group on the phenyl azide on the peptide silica azide, which destabilizes the singlet state of the nitrene intermediate formed. Other modes of attachment may have formed, but these cannot be confirmed until a solid-state ^{13}C NMR spectrum is produced of the peptide silica azide.

In all the silica azide reactions, there was the appearance of a small common peak at 87.5 ppm in the solid-state NMR spectra, probably due to a by-product of the reaction of the silica azides with water.

Suggestions for further work

In the immediate future, the ^{13}C solid-state NMR spectrum of unreacted peptide silica azide should be obtained to increase the understanding of the peptide silica azide + glutathione

spectrum by comparing the changes in both the spectra. Also, the ultraviolet absorbance spectrum of abscisic acid should be run to determine if its absorbance in solution would affect the photochemistry of the azide.

The ^{13}C solid-state NMR technique used is far from perfect – important information may be obscured by the broad and noisy NMR peaks, even after 28000 acquisitions of the spectra. Using a stronger magnet, more sensitive and finely tuned spectrometer would be a simple solution, but taking more advantage of solution-state NMR (whose peaks are very sharp) would be a good idea to extract information about each NMR peaks by running a solution-state NMR on a sample chemically similar to the silica azides and comparing with the solid-state spectrum of the supported azide. A disadvantage of this method is in reactions with the chemical of interest in solution, as excessive dimerization of free aryl azides (Lwowski 1970) are a problem as they darken the solution and may become the major reaction.

Another suggestion of further work is to analyse the immobilisation of simple molecules with few functional groups (e.g. ethene, methanoic acid) to the silica azide to elucidate and quantify the possible interactions. This would be very different to traditional solution-state azide chemistry in the literature as the azide groups have shown they are unlikely to dimerize when attached to the silica supports in this study, and would open up a new combinatorial chemistry approach to the immobilization problem.

References

SDBS, Integrated Spectral Data Base System for Organic Compounds.

Bellamy, L. J. (1995). The Infrared Spectrum of Complex Molecules, Chapman & Hall.

Dey and Harbourne Plant Biochemistry, Associated Press.

Fleming, S. A. (1995). "Chemical Reagents in Photoaffinity Labelling." Tetrahedron **51**(46): 12479-12520.

Heldt, H.-W. Plant Biochemistry & Molecular Biology, Oxford.

Levitt, M. L. (2003). Spin Dynamics: Basics of Nuclear Magnetic Resonance, Wiley.

Lwowski, W. (1970). Nitrenes, Interscience
Wiley.

Platz, M. S. (1995). "Comparison of Phenylcarbene and Phenylnitrene." Acc. Chem. Res. **28**: 487-492.

Sche, P. P., K. M. McKenzie, et al. (1999). "Display cloning: function identification of natural product receptors using cDNA-phage display." Chemistry & Biology **6**(10): 707-716.

Uttamchandani, M., P. W. Walsh, et al. (2005). "Small molecule microarrays: recent advances and applications." Curr. Op. Chem. Bio. **2005**(9): 4-13.

Appendix

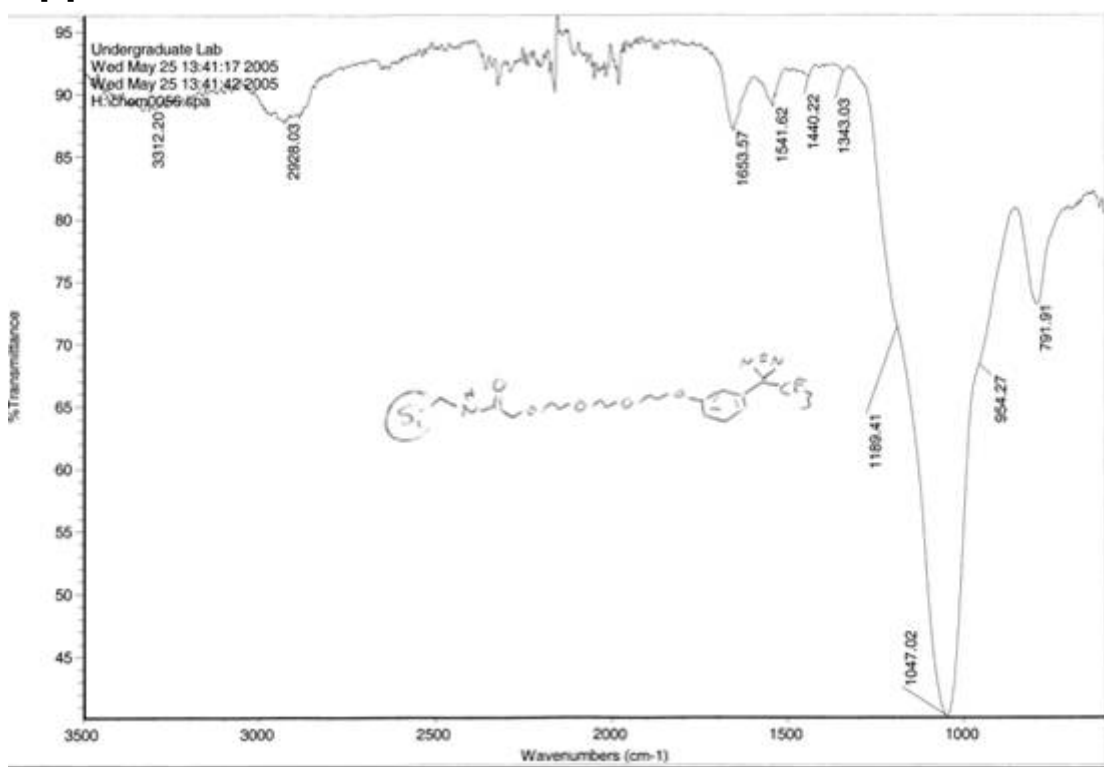


Figure 29: IR spectrum of SJD-IV-707.

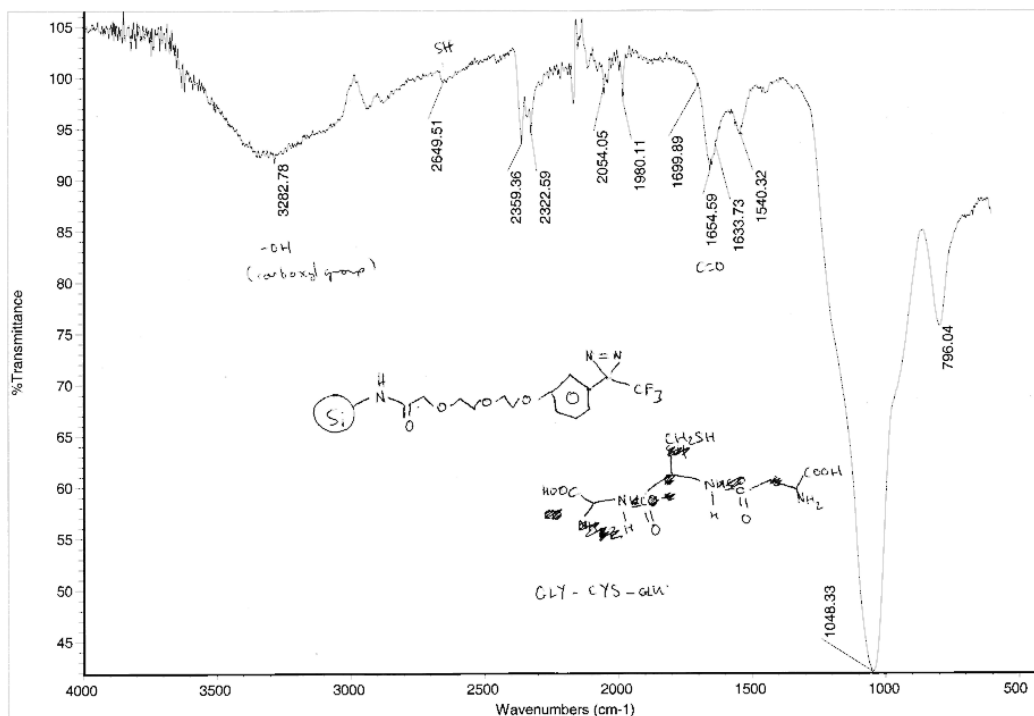


Figure 30: IR spectrum of SJD-IV-707 + glutathione + water.

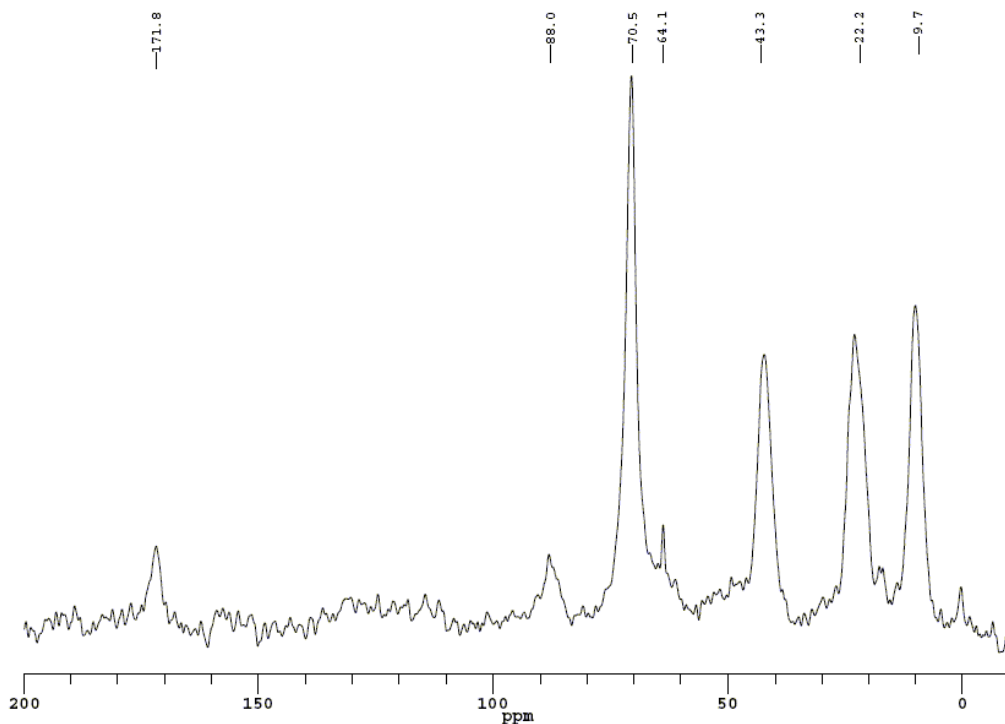


Figure 31: ^{13}C solid-state NMR spectrum of SJD-IV-707 + glutathione + water.

Table 5: Details of the ^{13}C solid-state spectrum of SJD-IV-707 + glutathione + water.

Spin speed	8kHz
Number of acquisitions Number of 'experiments' performed	23800
FID acquisition time length	40ms
Pulse delay (delay between acquisitions) Length of one 'experiment'	3s
90° ^1H pulse length (corresponding to 100kHz nutation frequency – to rotate all proton spins 90°)	$2.5\mu\text{s}$
Cross-polarisation contact time (pulse length of cross-polarisation pulses to transfer magnetism of ^1H to ^{13}C nuclei)	1ms

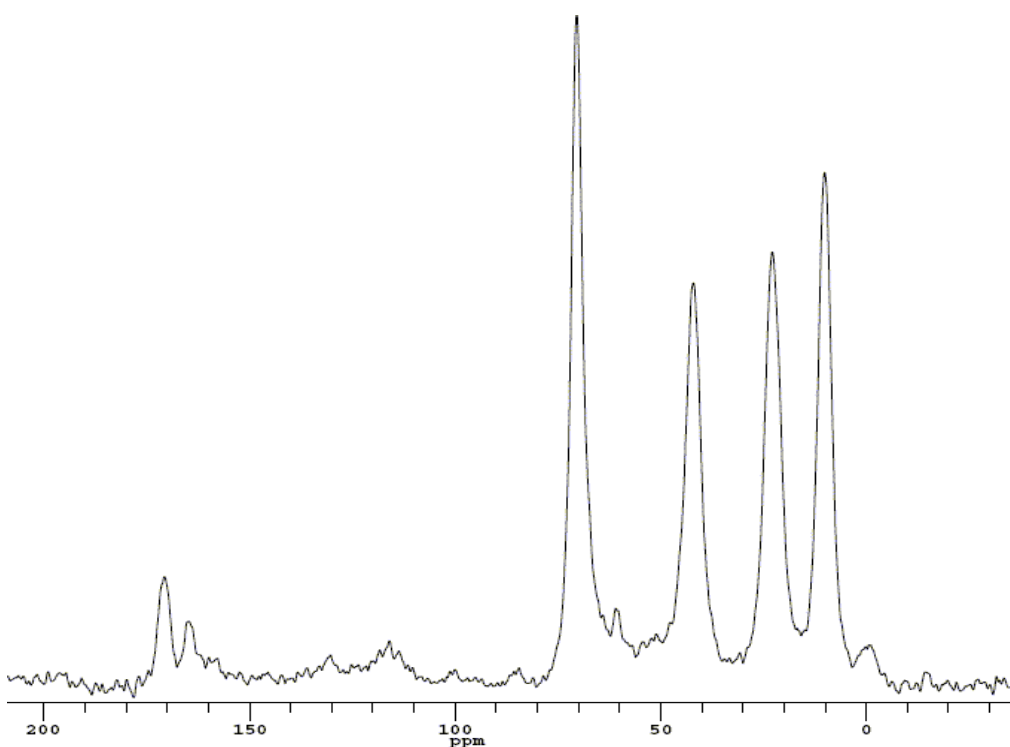


Figure 32: ^{13}C solid-state NMR spectrum of SJD-IV-707

Spin speed	8kHz
No. of acq.	24800
FID acq. time length	40ms
Pulse delay	3s
90° ^1H pulse length	$2.5\mu\text{s}$
CP contact time	1ms

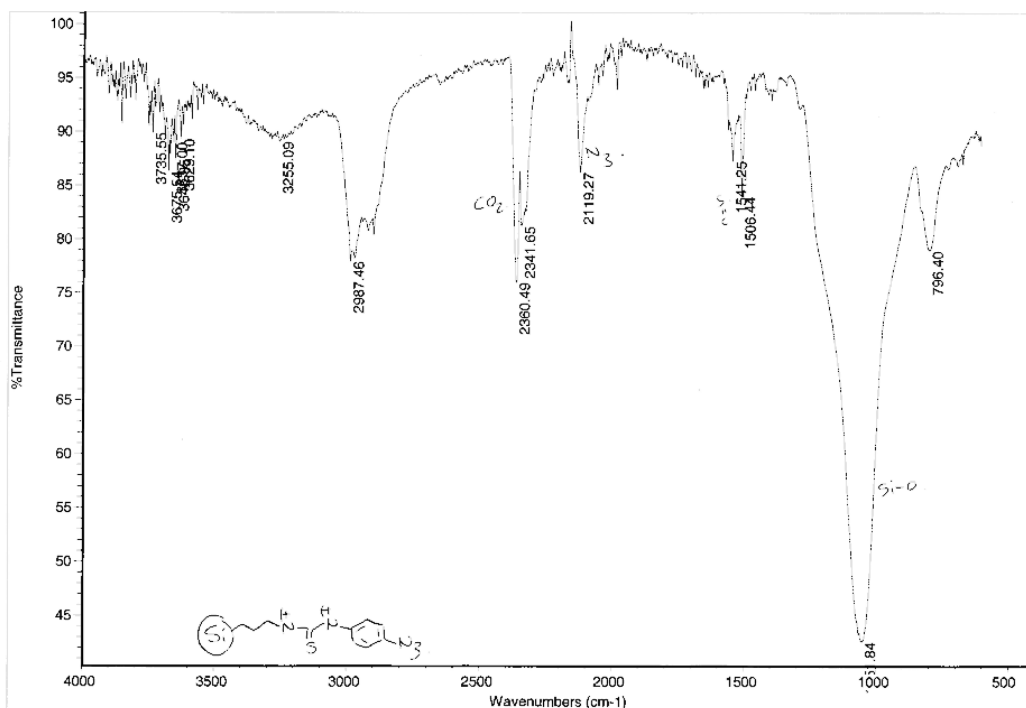


Figure 33: IR spectrum of unreacted thiourea silica azide.

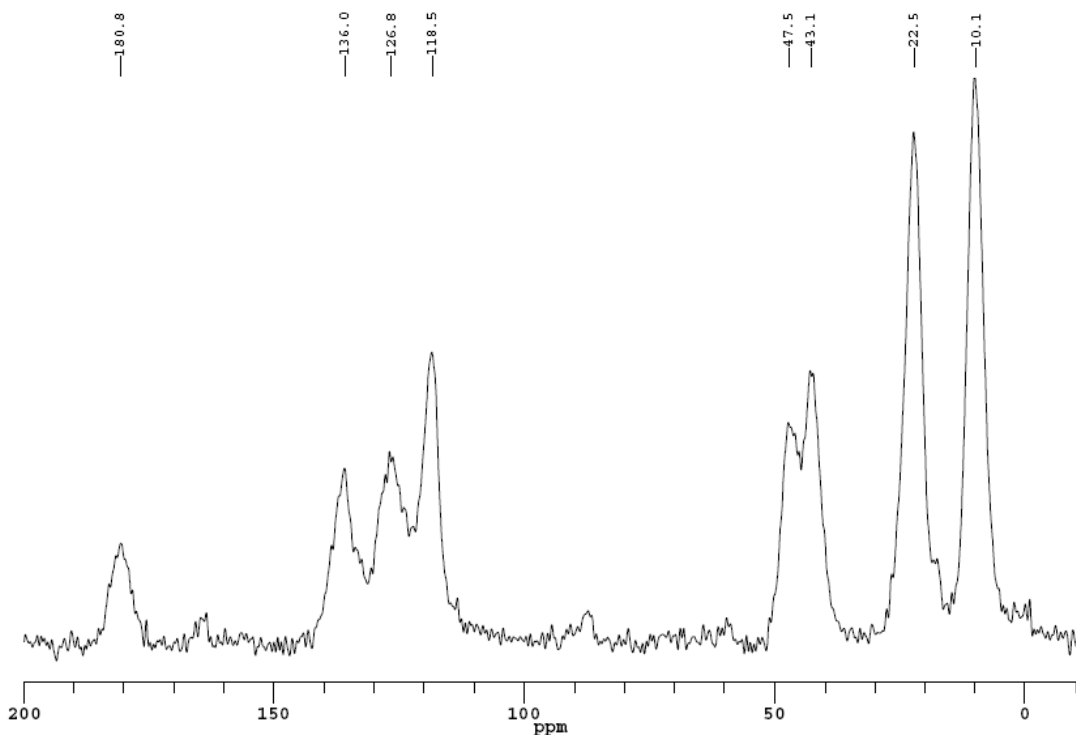


Figure 34: ¹³C solid-state NMR spectrum of unreacted thiourea silica azide.

Spin speed	8kHz
No. acq.	24088
FID acq. time length	40ms
Pulse delay	3s
90° 1H pulse length	2.5μs
CP contact time	1ms

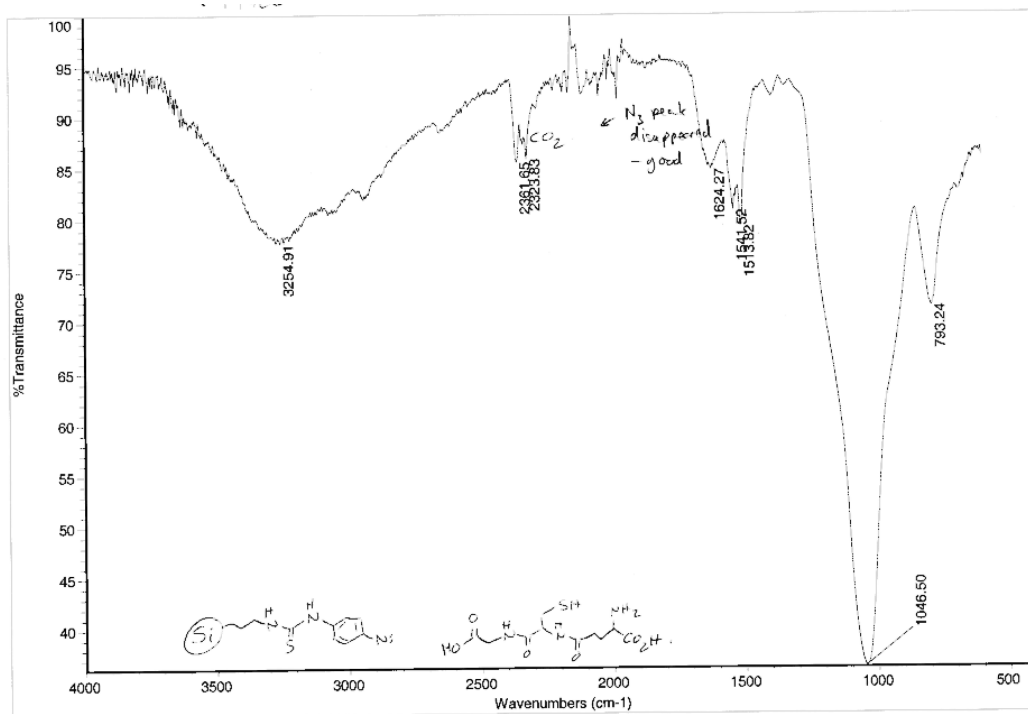


Figure 35: IR spectrum of thiourea silica azide + glutathione + water.

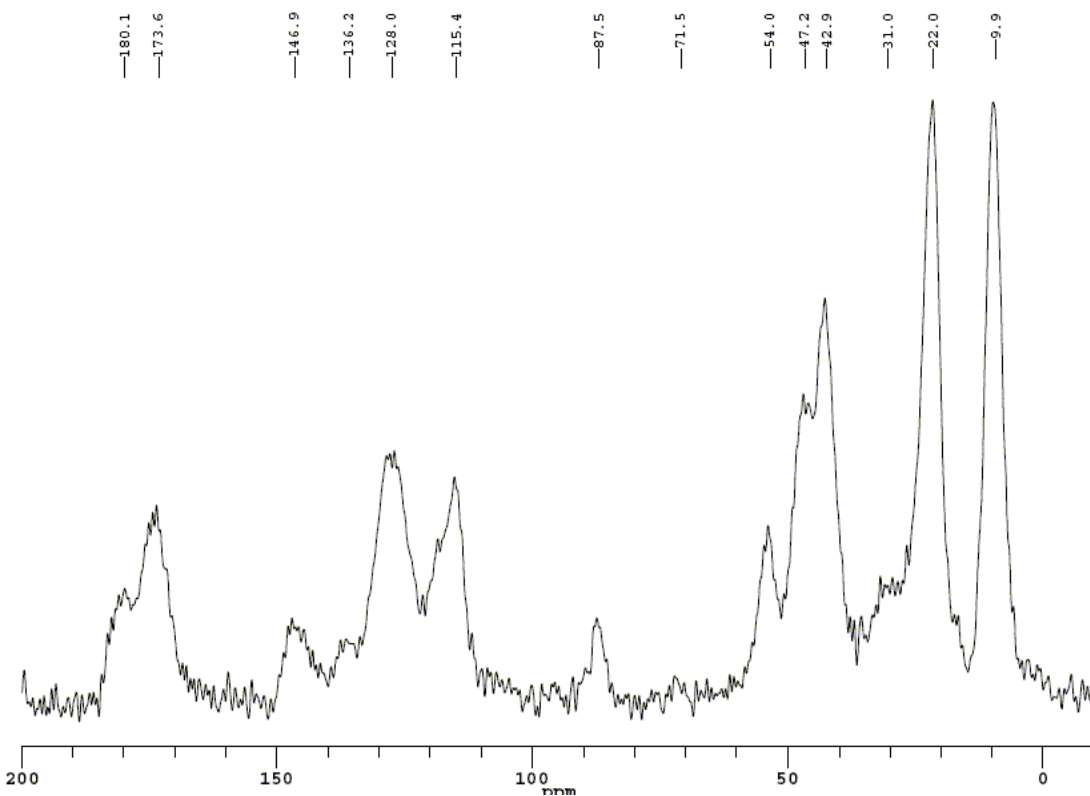


Figure 36: ¹³C solid-state NMR spectrum of thiourea silica azide + glutathione + water.

Spin speed	8kHz
No. acq.	24880
FID acq. time length	40ms
Pulse delay	3s
90° 1H pulse length	2.5μs
CP contact time	1ms

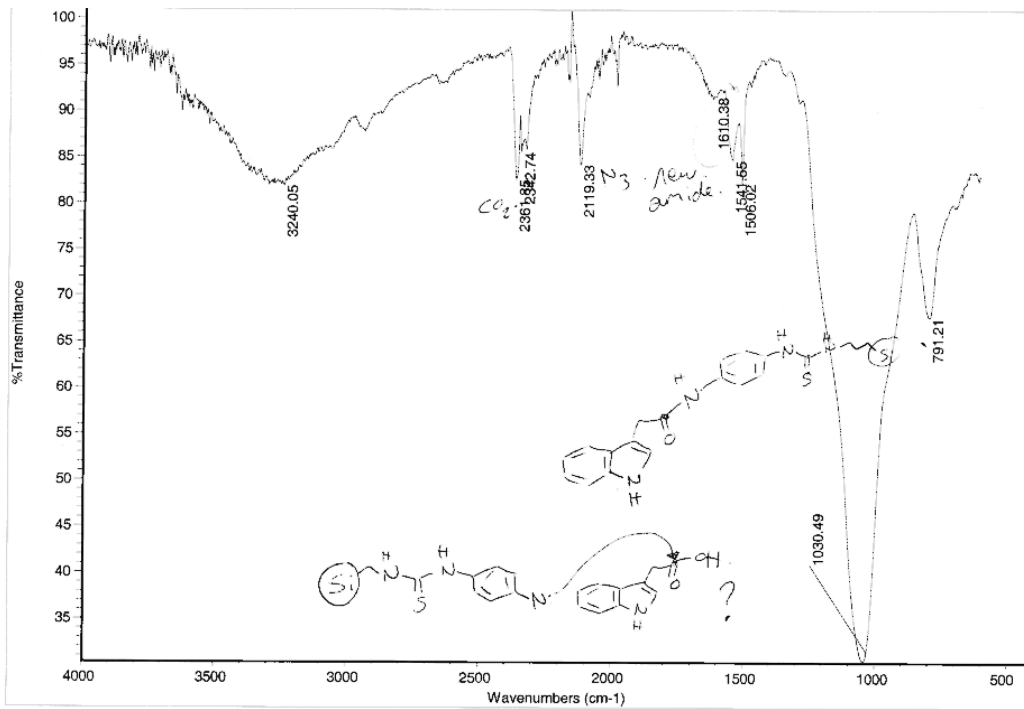


Figure 37: IR spectrum of thiourea silica azide + IAA + water.

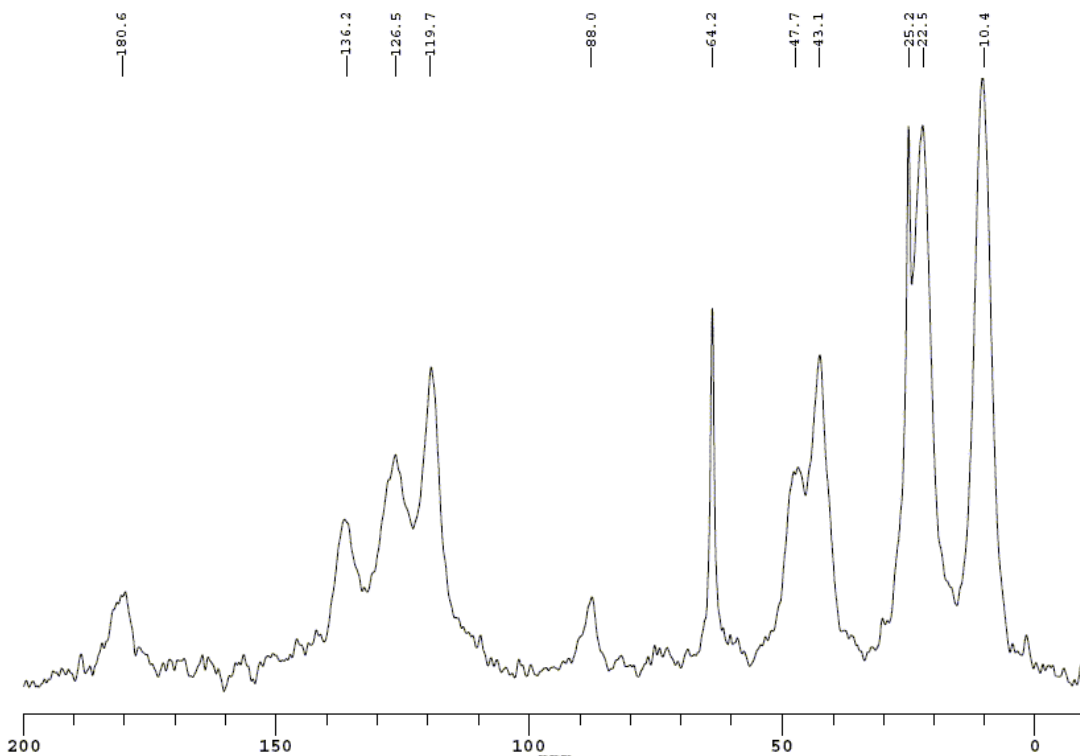


Figure 38: ^{13}C solid-state NMR spectrum of thiourea silica azide + IAA + water

Spin speed	8kHz
No. acq.	24800
FID acq. time length	40ms
Pulse delay	3s
90° ^1H pulse length	$2.5\mu\text{s}$
CP contact time	1ms

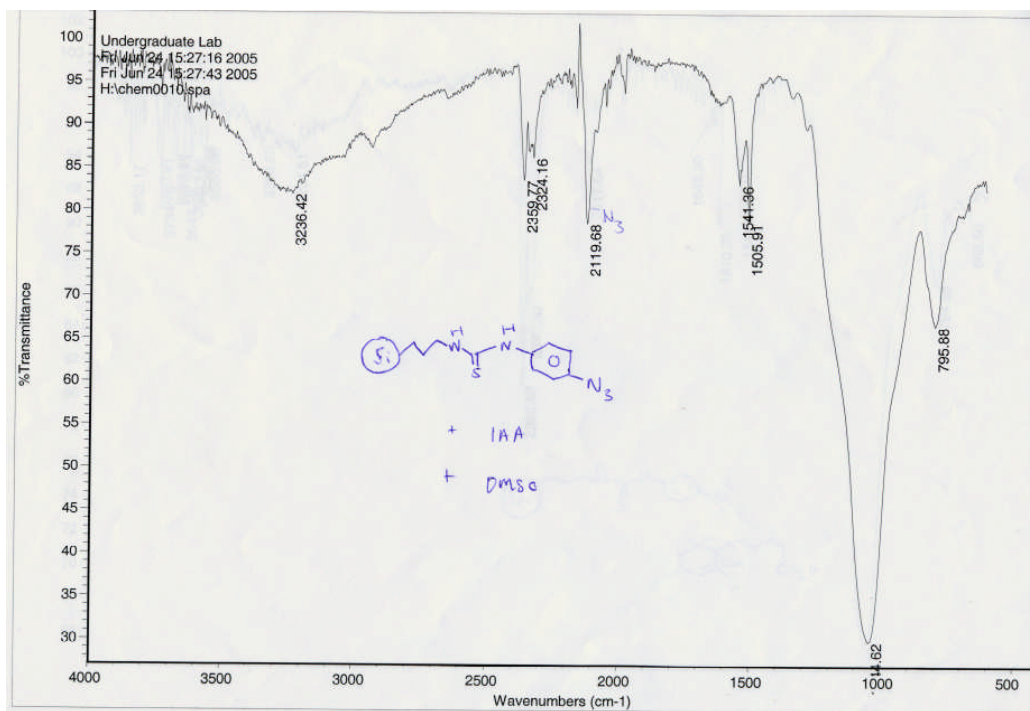


Figure 39: IR spectrum of thiourea silica azide + IAA + DMSO.

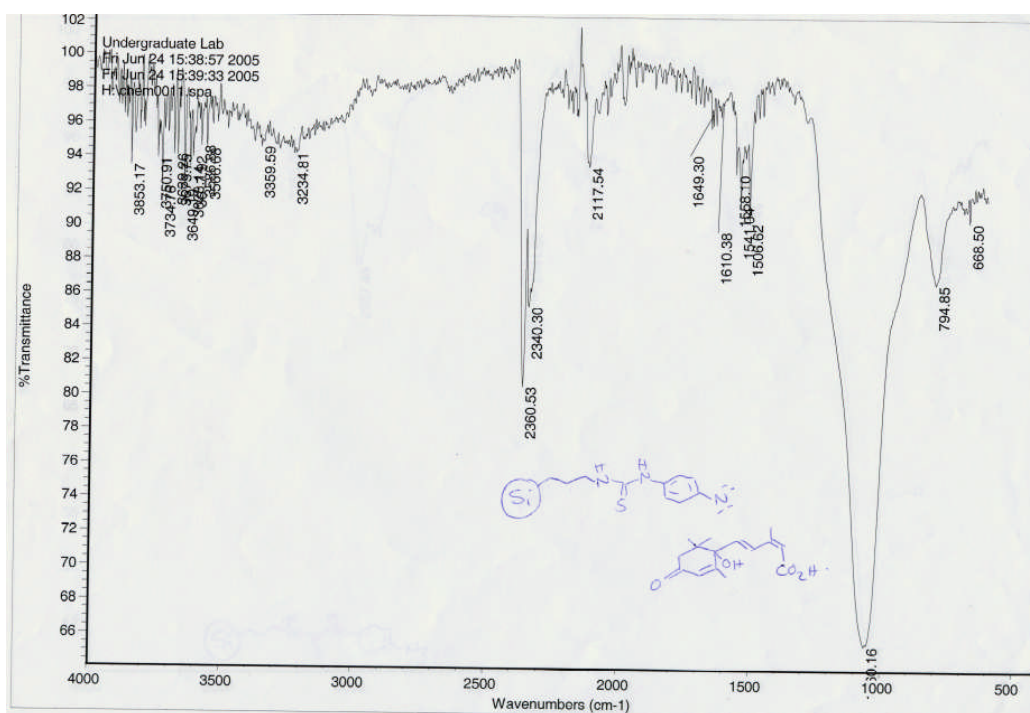


Figure 40: IR spectrum of thiourea silica azide + ABA + water + 20 drops DMSO.

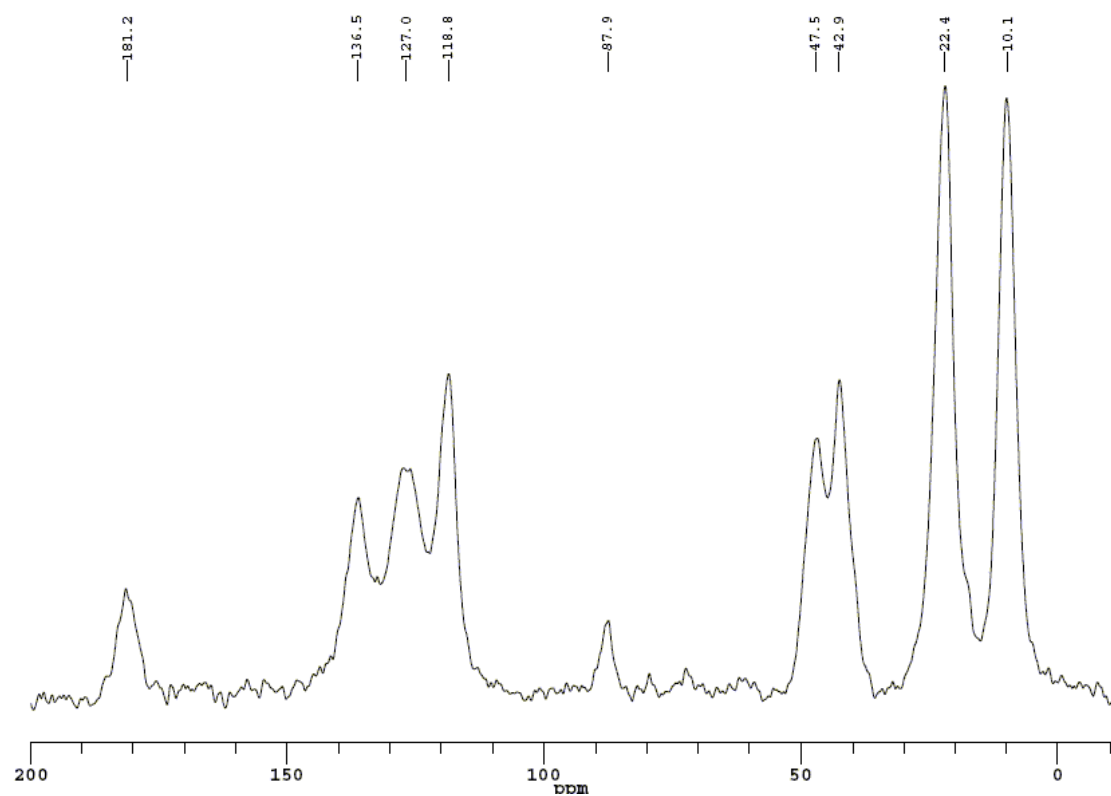


Figure 41: ^{13}C solid-state spectrum of thiourea silica azide + ABA + water + 20 drops DMSO

Spin speed	8kHz
No. acq.	27200
FID acq. time length	40ms
Pulse delay	3s
90° ^1H pulse length	$2.5\mu\text{s}$
CP contact time	1ms

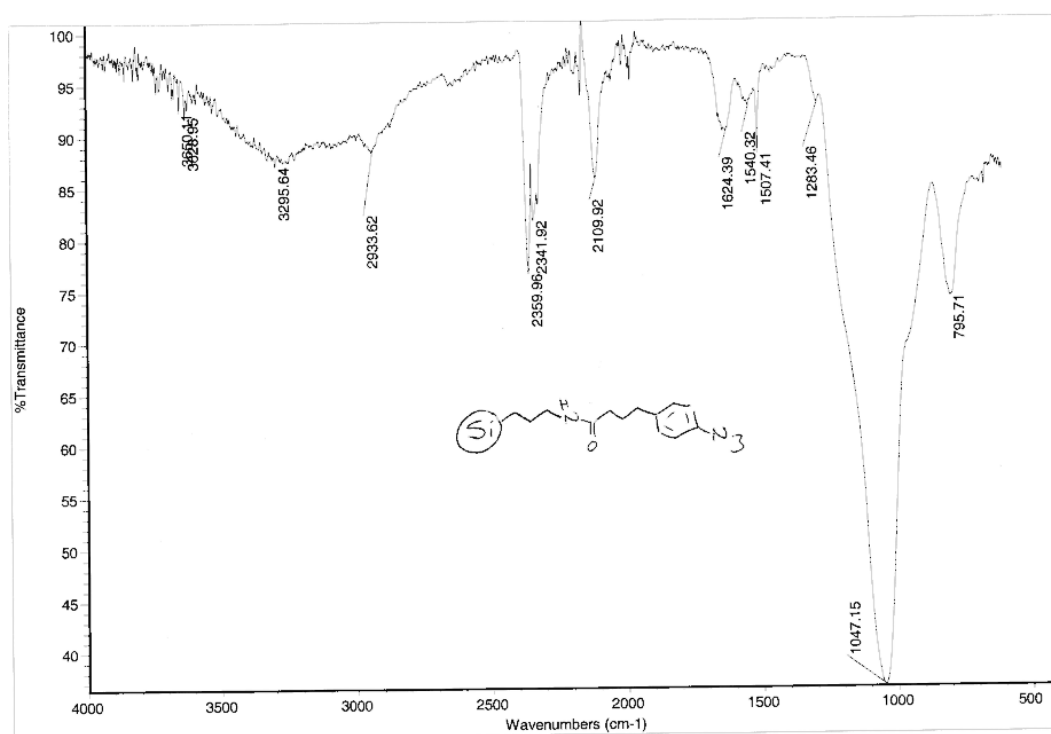


Figure 42: IR spectrum of unreacted peptide silica azide.

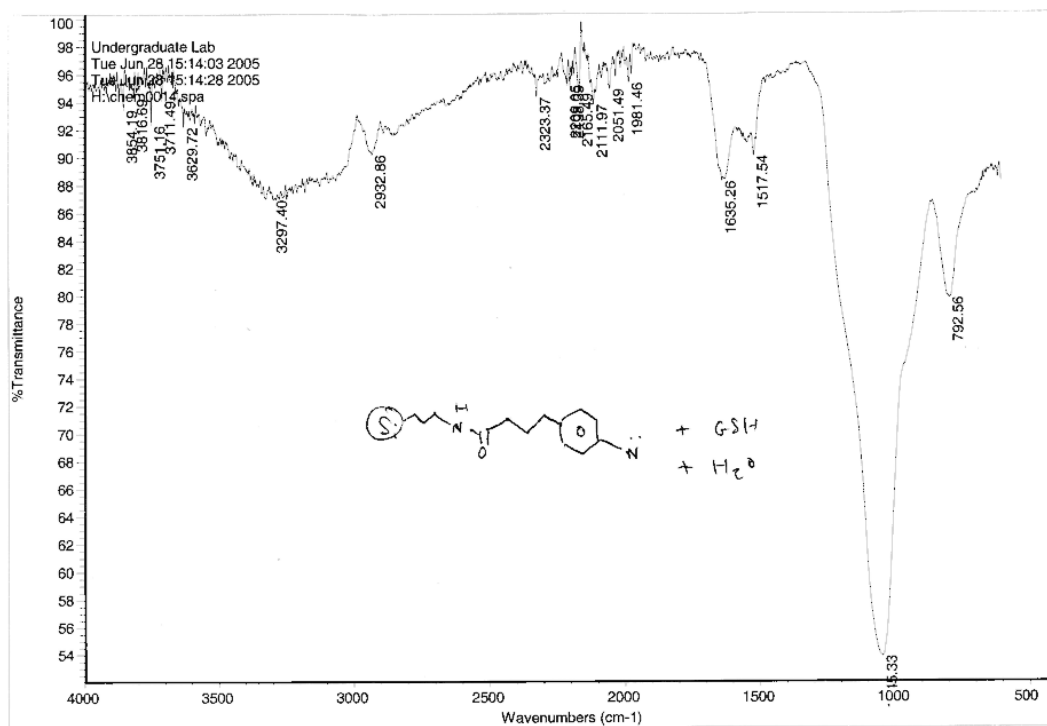


Figure 43: IR spectrum of peptide silica azide + glutathione + water.

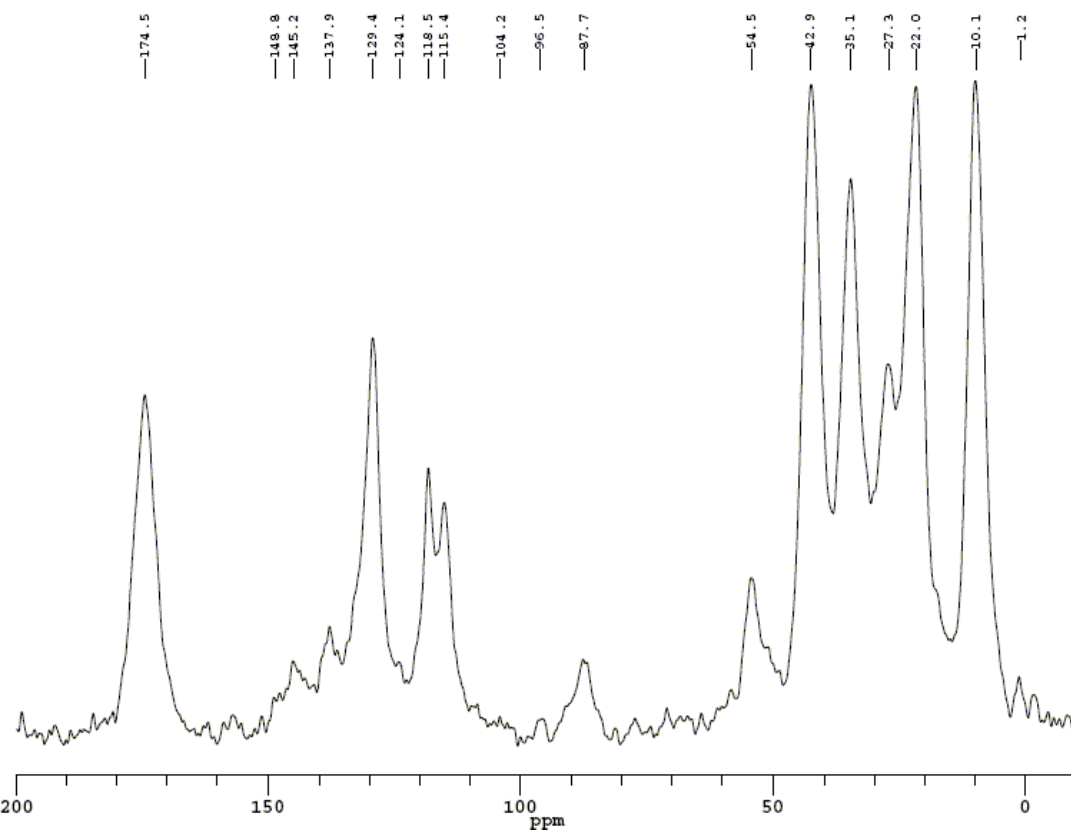


Figure 44: ¹³C solid-state NMR spectrum of peptide silica azide + glutathione + water.

Spin speed	8kHz
No. acq.	19000
FID acq. time length	40ms
Pulse delay	3s
90° 1H pulse length	2.5μs
CP contact time	1ms

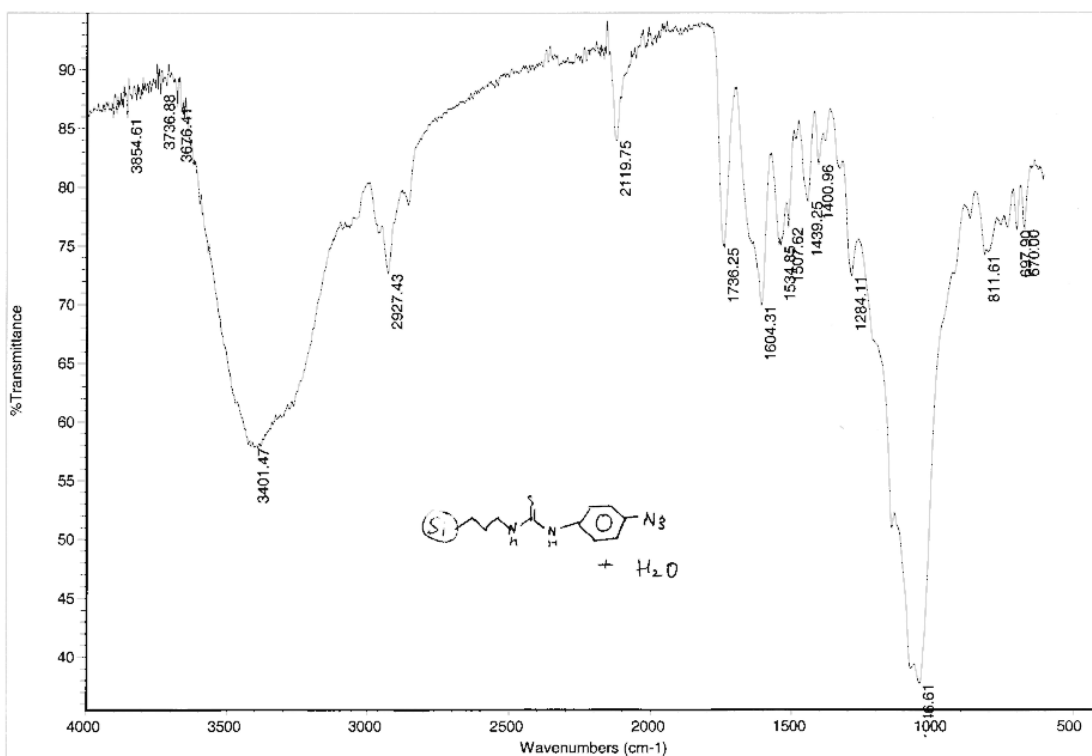


Figure 45: IR spectrum of silica azide + water.

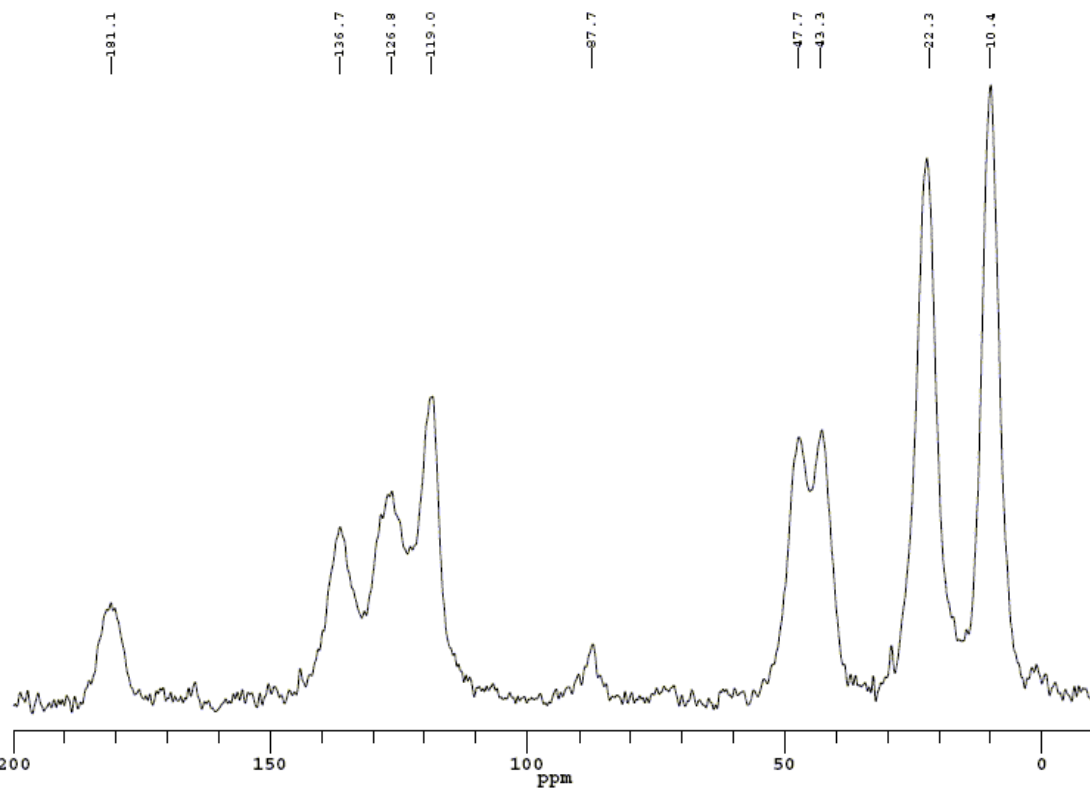


Figure 18: ¹³C solid-state NMR spectrum of silica azide + water.

Spin speed	8kHz
No. acq.	25000
FID acq. time length	40ms
Pulse delay	3s
90° 1H pulse length	2.5μs
CP contact time	1ms

Abbreviations

ABA	Abscisic acid
ATR	Attenuated Total Reflection
cDNA	Complementary deoxyribonucleic acid
CP	Cross-polarisation
DMSO	Dimethyl sulfoxide
FID	Free-induction decay
FTIR	Fourier Transform Infrared
GSH	Glutathione
IAA	Indole acetic acid
IR	Infrared
MAS	Magic-angle spinning
mRNA	Messenger ribonucleic acid
NOE	Nuclear Overhauser effect
NMR	Nuclear Magnetic Resonance
PEG	Polyethylene glycol (chain)
ppm	Parts per million
TMS	Tetramethylsilane
TPPM	Two-particle phase modulation
UV	Ultraviolet